Dear editor,

Here we submit our revised manuscript for consideration to be published on **Atmospheric Chemistry and Physics**

The further information about our manuscript is as follows:

Topic: Developing a novel hybrid model for the estimation of surface 8-h ozone (O_3) across the remote Tibetan Plateau during 2005-2018

Type of Manuscript: article

Authors: Rui Li[a], Yilong Zhao[a], Ya Meng[a], Wenhui Zhou[a], Ziyu Zhang[a], Hongbo Fu[a-c] [*]

 *Corresponding author:

Hongbo Fu; Address: Department of Environmental Science and Engineering, Fudan University, Shanghai 200433, China; Tel.: (+86)21-5566-5189; Fax: (+86)21-6564-2080; Email: fuhb@fudan.edu.cn

Firstly, we acknowledge the suggestions of editor and two reviewers, and are also grateful to your efficient serving. We have updated the manuscript on the basis of these valuable comments. Our responses were listed as following:

Reviewer #1: The subject is appropriate to Atmospheric Chemistry and Physics. This paper developed a novel hybrid model named random forest-generalized additive model (RF-GAM) to estimate the surface 8-h O_3 levels across the remote Tibetan Plateau during 2005-2018. This model displayed excellent prediction performances of O_3 spatiotemporal variations when compared with other seven machine learning models, and can be applied in the remote regions with sparse monitoring sites. This study is a valuable work. Therefore, I recommend clearly the acceptance for publication of this manuscript after revisions. Several editorial comments for improving the information content and presentation of the paper are listed as follows:

Response: Thank for reviewer's suggestions. I have revised the manuscript carefully based on reviewer's suggestions.

Comment 1: When you analyzed spatiotemporal variations of simulated 8-h O_3 concentrations and nonattainment days at the monitoring sites, why do you not use observed values for comparison? It may verify the results and rich your discussions.

Response: I agree with reviewer's suggestion. The measured mean 8-h O_3 concentrations were

added in Table 4. The relationships between measured O_3 concentrations and simulated O_3 levels have been added in the discussion part.

Comment 2: Since Community Multiscale Air Quality (CMAQ) model and other three-dimensional models have been widely applied to the simulation of surface O_3 concentrations, you'd better add a paragraph to summarize these results and compare your results with others to reveal the superiority of your novel model by adding more references such as Eder, B., and S. Yu, 2006. A performance evaluation of the 2004 release of Models-3 CMAQ. Atmospheric Environment, 40: 4811-4824.

Response: Thank for reviewer's suggestion. We have added a paragraph to discuss the advantage of RF-GAM model developed in our study compared with previous studies. The detailed explanations are as follows:

To date, some previous studies also simulated the surface O_3 concentration in Tibetan Plateau using statistical models (Zhan et al., 2018). For instance, Zhan et al. (2018) employed the RF-STK model to estimate the surface O_3 concentration over China, and explained the 66% spatial variability of O_3 level in Tibetan Plateau. Apart from these statistical models, some classical CTMs were also applied to estimate the O_3 concentration in the remote area. Both of Liu et al. (2018) and Lin et al. (2018) used CMAQ to estimate the O_3 level across China, while the R^2 values in most of cities were lower than 0.50. In terms of the predictive performance, the RF-GAM model in our study showed the significant advantages compared with previous studies. It should be noted that our RF-GAM model could outperform most of current models, chiefly because of (1) accounting for the temporal autocorrelation of surface O_3 concentration; and (2) the use of high-quality satellite data.

Comment 3. As for the temporal variations of the simulated 8-h O_3 concentrations and nonattainment days as depicted in Fig. 7 and Fig. 10, the change pattern from 2005 to 2018 is not very obvious. Would you mind showing interannual variations in a clearer way?

Response: Thank for reviewer's suggestions. The interannual variation has been added in the Tab. S1, which was clearly shown in the form of table.

Comment 4. L225-227 Regarding the other five models (i.e., RF, generalized regression neutral

network (GRNN), backward propagation neural network (BPNN), Elman neural network (ElmanNN), and extreme learning machine (ELM)), you should put all related results from them into SI because you already prove that RF-GAM model is the best and it is unnecessary to present the results of other worse ones in the main text part.

Response: I agree with reviewer's suggestion. We have placed some other models in SI.

Comment 5. There are many English grammar errors in the manuscript. I only list some of them here for your reference below (please make all necessary corrections before publication).

Response: Thank for reviewer's suggestions. We have revised the grammar errors throughout the manuscript based on the reviewer's suggestions.

Comment 6. L16: It should be "to predict the surface 8-h O_3 concentrations: : :."

Response: I agree with reviewer's suggestion. "concentration" has been replaced by "concentrations".

Comment 7. L21: It should be "to predict the surface 8-h O_3 concentrations: : :.".

Response: We have corrected these errors based on reviewer's suggestions.

Comment 8. L25: It should be "the estimated O_3 mean concentrations: : :: : :"

Response: We have corrected these errors based on reviewer's suggestions.

Comment 9. L44: It should be "The chemical reactions between NO_x and VOCs in the presence of sunlight were: : :"

Response: We have corrected these errors based on reviewer's suggestions.

Comment 10. L85: It should be "the daily satellite data enable the fine-scale estimations of O_3 level: : :"

Response: We have corrected these errors based on reviewer's suggestions.

Comment 11. L90-91: It should be "the global distributions of O_3 concentrations based on simple linear : : :."

Response: We have corrected these errors based on reviewer's suggestions.

Comment 12. L103-104: It should be "can obtain the contributions of each predictor to air pollutants: : :."

Response: We have corrected these errors based on reviewer's suggestions.

Comment 13. L146-147: It should be "simulate the gridded 8-h O_3 concentrations over Tibetan Plateau for the first time: : :.".

Response: We have corrected these errors based on reviewer's suggestions.

Comment 14. L162: It should be "lack of anthropogenic activities and most of the residents focus on southeast and south parts of: : :"

Response: We have corrected these errors based on reviewer's suggestions.

Comment 15. L171: It should be "The data quality of all the monitoring sites was assured on.."

Response: We have corrected these errors based on reviewer's suggestions.

Comment 16. L175: It should be "The O_3 column amounts (DU) during 2005-2018 were downloaded from the Ozone Monitoring: : :".

Response: We have corrected these errors based on reviewer's suggestions.

Comment 17. L294-295: It should be "we also investigated the spatial variabilities of the predictive accuracy for RF-GAM model: : :..".

Response: We have corrected these errors based on reviewer's suggestions.

Comment 18. L337-337 about the effects of RH on the O_3 formation: Please add the following reference to have more discussions in terms of chemical mechanism: S. Yu, 2019. Fog geoengineering to abate local ozone pollution at ground-level by enhancing air moisture. Environ Chem Lett, 17(1), 565–580, doi: 10.1007/s10311-018-0809-5.

Response: We have corrected these errors based on reviewer's suggestions. Besides, we also citied the reference in the revised version.

Comment 19. L353-354: It should be "It was well known that photochemical reactions of BVOCs and NOx in the presence of sunlight were beneficial to the O3 formation..". Also please add more references about this such as: S. Yu, et al., 2006. Performance and diagnostic evaluations of a real-time ozone forecast by the Eta-CMAQ model suite during the 2002 New England Air Quality Study (NEAQS). Journal of the Air & Waste Management Association, 56:1459-1471.

Response: We have corrected these errors based on reviewer's suggestions. Besides, we also citied the reference in the revised version.

Comment 20. L397-398: It should be "Besides, the 8-h O_3 concentrations in Tibetan Plateau displayed significantly seasonal discrepancy: : :..".

Response: We have corrected these errors based on reviewer's suggestions.

Comment 21. P44: It should be "Table" in stead of "Tab.".

Response: We have corrected these errors based on reviewer's suggestions.

Comment 22. P2, L34: "shared with" => "shared"

Response: We have corrected these errors based on reviewer's suggestions.

Comment 23. P3, L62: "surfacce" => "surface"

Response: We have corrected these errors based on reviewer's suggestions.

Comment 24. P3, L63: It should be ": : :concentration displayed the gradual decrease in the recent ten years".

Response: We have corrected these errors based on reviewer's suggestions.

Comment 25. P4, L69: "lacks of" => "lacks"

Response: We have corrected these errors based on reviewer's suggestions.

Comment 26. P8, L163: "is consisted of" => "consists of"

Response: We have corrected these errors based on reviewer's suggestions.

Comment 27. P20, L422, 434: "Tab. 2" should be "Table 4"

Response: We have corrected these errors based on reviewer's suggestions.

Reviewer #2: This paper attempts to create a machine-learned statistical model to estimate 8-h surface ozone concentrations where few measurements exist (Tibetan plateau). The model formulation (RF-GAM) is interesting and the subject fits within the scope of ACP. There are several flaws with the presentation of this work, namely the lack of significance tests and alternate performance metrics in addition to English grammatical errors throughout. However, I am optimistic the authors can correct these issues and I believe this work will be a very important addition to the scientific literature of air pollution in rural regions.

Response: Thank for reviewer's suggestions. I have revised the manuscript based on the reviewer's suggestions carefully. The detailed responses are as follows:

Comment 1: Does the paper address relevant scientific questions within the scope of ACP? This paper attempts to create a machine-learned statistical model to estimate 8-h surface ozone concentrations for the Tibetan plateau. The RF-GAM model is interesting and the subject fits within the scope of ACP.

Response: Thank for reviewer's suggestions. The journal (ACP) focuses on the Earth's atmosphere and the underlying chemical and physical processes. The modelling of atmospheric components in the atmosphere is a hot topic of ACP, and many relevant references have been published in this journal. Therefore, we believe that the paper addresses relevant scientific questions within the scope

of ACP.

Comment 2: Does the paper present novel concepts, ideas, tools, or data? The machine learning model formulation is interesting and the application of the GAM to remove autocorrelation in the time series data is novel.

Response: Thank for reviewer's suggestions. The paper presents a novel machine learning model named RF-GAM, which shows excellent performance in predicting the 8-h O_3 concentration over Tibetan Plateau. The development of this model is the major novelty of this present study. Besides, the present study fills the gap of statistical estimation 8-h O_3 level in a remote region, and provides useful datasets for epidemiological studies and air quality management. The implication is very important. Moreover, we also

Comment 3: Are substantial conclusions reached? Not particularly, the performance metrics presented in the work are not convincing. The authors present RMSE as an absolute measure of performance yet the best performing model had an RMSE of 14.41 $\mu g/m^3$, which is greater than 10% error relative to the WHO 8-h ozone critical value (100 $\mu g/m^3$) they are using to determine nonattainment. There is very little discussion about significant differences between performance due to model architecture and between seasons and years. Greater discussion of model uncertainty needs to be had. This study addresses an important topic that lacks much attention in scientific literature, but the performance of the model is still considerably lacking.

Response: Thank for reviewer's suggestions. The differences of performance between years has been added in the Table 1. The predictive performances in different seasons were also shown in Table 2. The contents have been expanded to discuss the temporal variation of predictive accuracy of O_3 concentration. The uncertainty of the present study is also added in the revised version: "The determination of nonattainment days showed some uncertainties owing to the predictive error of modelled O_3 concentration. First of all, meteorological data used in RF-GAM model were collected from reanalysis data and these gridded data often showed some uncertainties, which could increase the uncertainty of O_3 estimation. Second, the O_3 column amount used in the present study reflected vertical O_3 column amount rather than surface O_3 concentration. Thus, it could decrease the predictive performance of surface O_3 level". Besides, some important references were also added in the revised version.

Comment 4: Are the scientific methods and assumptions valid and clearly outlined? Scientific

methods and data preprocessing are outlined well. Figure 2 presents a workflow method for the machine learning model, though including an actual architectural schematic of the final model would be better (e.g. what does the random forest look like in terms of the number of trees, nodes, etc.). Furthermore, none of the other machine learning models were given an architectural model description, i.e., how many nodes in the neural network, activation functions, etc. Machine learning is a burgeoning field with many nascent applications. Therefore, this paper would benefit going into greater detail about what other machine learning methods they tried in detail so that others could learn from their attempts.

Response: Thank for reviewer's suggestions. We have added some detailed information especially key parameters about various machine learning models in the revised version. Based on the iteration result, the optimal n_{tree} and m_{try} reached 500 and 5, respectively. For XGBoost method, the optimal tree depth and minimum child weight was set as 8 and 6, respectively. The activation functions of GRNN, BPNN, and ElmanNN were sigmoid function. The number of nodes in BPNN and ElmanNN were 5 and 4, respectively. The number of nodes in GRNN was equal to the sample size.

Comment 5: Are the results sufficient to support the interpretations and conclusions? (cite sections) There must be a greater statistical argument presented to support the interpretations of the authors. Oftentimes the authors present only an R^2 metric or an RMSE value to evaluate the goodness of fit among conditions. These performance measures are relatively obfuscating as even though ozone might increase or decrease between temporal/spatial extents, these changes, I suspect, are statistically insignificant. There are practically no significance tests conducted. These performance metrics must be put into greater context. Perhaps including confidence intervals (rather than only standard deviations) would also help. For the variable importance section 3.2, the authors should present an error covariance matrix for the inputs. For random forest algorithms, the variable importance determined by the model is meaningless if the variables are co-linear. Furthermore, oftentimes the explanations for the concentration of ozone are too speculative (e.g. lines 334-351). There are numerous mentions of NO_x and VOCs contributing to ozone loss or formation, yet this analysis cannot address such concerns directly as the model does not take into account these variables. These explanations are well thought out but exceed the scope of what this model can answer. Perhaps place them in the discussion rather than with the results. In addition to RMSE, an absolute metric, perhaps the authors should consider reporting a relative metric such as percent error

in tandem. R^2 values of 0.60 and RMSE values of 14 $\mu g/m^3$ are not readily obvious/interpretable if this is adequate performance. Also, conducting significance tests between different models might be beneficial. I am not convinced that RF and XGBoost are markedly different. The addition of the GAM seems like a different model architecture than typical machine learning models. That is, why not attach the GAM to the XGBoost and see how that performs? It is fine if the authors wanted to create an RF-GAM model from the outset, but the comparison between the other models does not seem very robust.

Response: Thank for reviewer's suggestions. We employed one-way ANOVA method to compare the predictive values of eight models. The results are as follows:

Source	SS	df	MS	F	p value
Groups	24542.6	7	3506.09	9.01	<0.01
Error	59209467.7	152154	389.14		
Total	59234010.3	152161			

Based on the result of one-way ANOVA, we found that the RF-GAM model showed significantly better predictive performance compared with other seven models.

Indeed, the traditional statistical model required that all of the independent variables should be deviated from the autocorrelation. The multicollinearity of variables might decrease the reliability of these models. However, the random forest method did not consider the autocorrelation of all the variables because the algorithm was nonlinear.

Indeed, some explanations for the concentration of ozone were speculative, and thus we revised many redundant or speculative explanations especially for the contribution of NO_x and VOCs to ozone formation. However, some explanations were well-founded because it could be supported by the Fig. S4. Besides, the effects of meteorological factors on ozone formation were confirmed by some previous studies and Fig. S5-S11, which was reliable.

In addition to RMSE, we also added a new indicator named relative prediction error (RPE) to assess the predictive accuracy (Fig. 3 and Fig. 4). We have employed the XGBoost method to combine the GAM to estimate the surface O_3 concentration (see the following figure), and found that the hybrid model showed the worse performance compared with RF-GAM model. The R^2 value of XGBoost-GAM model was significantly lower than that of RF-GAM model. Besides, both of

RMSE and MPE for XGBoost-GAM model were also significantly higher than those of RF-GAM. Thus, we believed that RF-GAM was more appropriate to estimate the O_3 concentration in Tibetan Plateau.
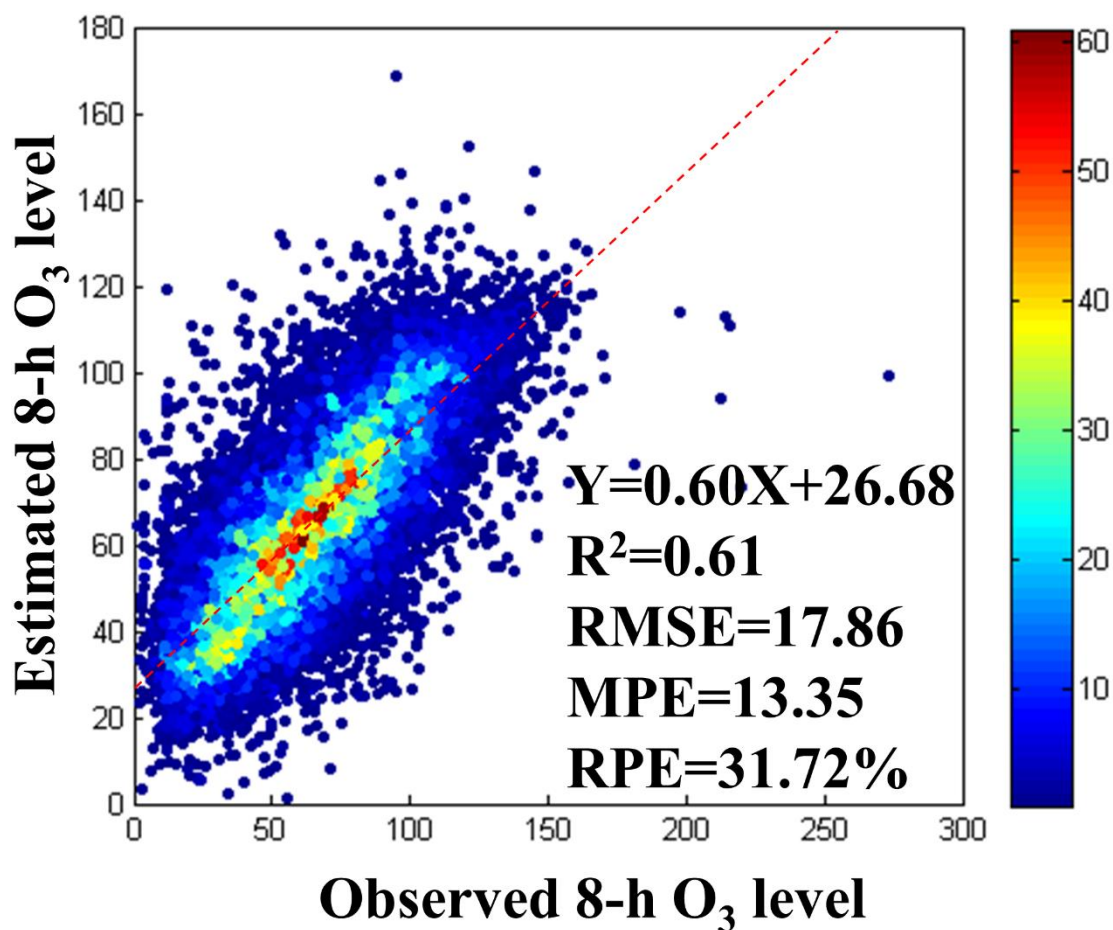
Comment 6: Is the overall presentation well structured and clear? The overall structure and flow of the paper are coherent, though oftentimes the English is not clear.

Response: Thank for reviewer's suggestion. We have significantly revised the language throughout the paper.

Comment 7: Is the language fluent and precise? This study needs considerable corrections to numerous grammatical and language errors. There are far too often awkward phrasings and mixed tenses.

Response: Thank for reviewer's suggestion. We have significantly revised the language throughout the paper and corrected many grammar errors.

Comment 8: Should any parts of the paper (text, formulae, figures, tables) be clarified, reduced, combined, or eliminated? Many of the figures are too small to view. Needs to be increased in size.

Response: I agree with reviewer's suggestions. We have redrawn the Fig. 7 and Fig. 10 to increase the figure size.

Comment 9: Are the number and quality of references appropriate? Great overview and command of the literature.

Response: Thank for reviewer's suggestions. We have added some latest references in the revised version though many relevant references have been added.

Following are some line comments, though not all-inclusive:

Comment 10: a few times you use the word 'beneficial' to describe conditions that create pollution, perhaps consider different word choices as this is a bit awkward.

Response: I agree with reviewer's suggestions. "beneficial" was changed into "caused", "triggered", or "promoted".

Comment 11: Also found on line 127. 102-103: "decision tree models such as random forest (RF) and extreme gradient boosting (XGBoost) strike a perfect balance between prediction performance and computing cost". This seems to be a wide sweeping claim without a reference. Decision trees may be faster to train than neural networks, but they are also slower to evaluate. That is, decision trees are slow to train and slow to test, whereas neural networks are very slow to train and very fast to test. Consider revising your claim.

Response: I agree with reviewer's suggestions. (Line 102-103) The sentence has been changed into "Among these machine learning algorithms, decision tree models such as random forest (RF) and extreme gradient boosting (XGBoost) generally showed fast training speed and excellent prediction accuracy".

Comment 12: 135-138: awkward, confusing phrasing

Response: Thank for reviewer's suggestions. (Line 136-139) The sentence has been changed into "Unfortunately, these scarce monitoring sites in Tibetan Plateau cannot capture real O_3 pollution status especially in the remote areas (e.g., Northern part of Tibetan Plateau) because each site only possessed limited spatial representativeness".

Comment 13: Line 190: Still not sure why you included GDP as an input variable. You write that you integrated it because "these data were available each five years". Please provide a scientific explanation for the inclusion of this variable.

Response: Thank for reviewer's suggestion. GDP was included in the original model because many

previous studies confirmed that GDP might be linked with the O_3 pollution (Li et al., 2020 JCP). It was well known that the hotspot of O_3 pollution focused on the area with the higher VOCs and NO_x (e.g., industrial points and residential areas). These regions often displayed the relatively higher GDP compared with other regions.

1 **Developing a novel hybrid model for the estimation of surface 8-h ozone (O₃) across the**

2 **remote Tibetan Plateau during 2005-2018**

3 Rui Li[a], Yilong Zhao[a], Ya Meng[a], Wenhui Zhou[a], Ziyu Zhang[a], Hongbo Fu[a-c] *

4 *[a] Shanghai Key Laboratory of Atmospheric Particle Pollution and Prevention, Department of*

5 *Environmental Science & Engineering, Institute of Atmospheric Sciences, Fudan University,*

6 *Shanghai, 200433, P.R. China*

7 *[b] Collaborative Innovation Center of Atmospheric Environment and Equipment Technology*

8 *(CICAEET), Nanjing University of Information Science and Technology, Nanjing 210044, P.R.*

9 *China*

10 *[c] Shanghai Institute of Pollution Control and Ecological Security, Shanghai 200092, P.R. China*

11 **Corresponding author**

12 fuhb@fudan.edu.cn

13 **Abstract**

14 We developed a two-stage model named random forest-generalized additive model (RF-GAM)

15 based on satellite data, meteorological factors, and other geographical covariates to predict the

16 surface 8-h O₃ concentrations across the remote Tibetan Plateau. The 10-fold cross-validation result

17 suggested that RF-GAM showed the excellent performance with the highest R^2 value (0.76) and

18 lowest root mean square error (RMSE) (14.41 μg/m³) compared with other seven machine learning

19 models. The predictive performance of RF-GAM model showed significantly seasonal discrepency

20 with the highest R^2 value observed in summer (0.74), followed by winter (0.69) and autumn (0.67),

21 and the lowest one in spring (0.64). Additionally, the unlearning ground-observed O₃ data collected

22 from open websites were applied to test the transferring ability of the novel model, and confirmed

23 that the model was robust to predict the surface 8-h O_3 concentration during other periods ($R^2 = 0.67$,

24 RMSE = 25.68 µg/m³). RF-GAM was then used to predict the daily 8-h O_3 level over Tibetan

25 Plateau during 2005-2018 for the first time. It was found that the estimated O_3 concentrations

26 displayed a slow increase from 64.74 ± 8.30 µg/m³ to 66.45 ± 8.67 µg/m³ from 2005 to 2015,

27 whereas it decreased from the peak to 65.87 ± 8.52 µg/m³ during 2015-2018. Besides, the estimated

28 8-h O_3 concentrations exhibited notably spatial variation with the highest values in some cities of

29 North Tibetan Plateau such as Huangnan (73.48 ± 4.53 µg/m³) and Hainan (72.24 ± 5.34 µg/m³),

30 followed by the cities in the central region including Lhasa (65.99 ± 7.24 µg/m³) and Shigatse (65.15

31 ± 6.14 µg/m³), and the lowest one in a city of Southeast Tibetan Plateau named Aba (55.17 ± 12.77

32 µg/m³). Based on the 8-h O_3 critical value (100 µg/m³) scheduled by World Health Organization

33 (WHO), we further estimated the annually mean nonattainment days over Tibetan Plateau. It should

34 be noted that most of the cities in Tibetan Plateau shared ~~with~~ the excellent air quality, while several

35 cities (e.g., Huangnan, Haidong, and Guoluo) still suffered from more than 40 nonattainment days

36 each year, which should be paid more attention to alleviate local O_3 pollution. The result shown

37 herein confirms the novel hybrid model improves the prediction accuracy and can be applied to

38 assess the potential health risk, particularly in the remote regions with sparse monitoring sites.

39 **Keywords:** Surface O_3 level; satellite data; random forest; generalized additive model; Tibetan

40 Plateau

41 **1. Introduction**

42 Along with the rapid economic development and urbanization, the anthropogenic emissions of

43 nitrogen oxides (NO_x) and volatile organic compounds (VOCs) displayed high-speed growth. The

44 chemical reactions between NO_x and VOCs in the presence of sunlight ~~was beneficial to~~triggered

45   the ambient ozone (O_3) formation (Wang et al., 2019; Wang et al., 2017). As a strong oxidant,

46   ambient O_3 could play a negative role on human health through aggravating the cardiovascular and

47   respiratory function (Ghude et al., 2016; Marco, 2017; Yin et al., 2017a). Apart from the effect on

48   human health, O_3 also posed a great threaten on vegetation growth (Emberson, 2017; Feng et al.,

49   2015; Qian et al., 2018; Feng et al., 2019). Moreover, the tropospheric O_3 can perturb the radiative

50   energy budget of the earth-atmosphere system as the third most important greenhouse gas next to

51   carbon dioxide (CO_2) and methane (CH_4), thereby changing the global climate (Bornman et al.,

52   2019; Fu et al., 2019; Wang et al., 2019). Recently, the particulate matter less than 2.5 μm ($PM_{2.5}$)

53   concentration showed the persistent decrease, while the O_3 issue has been increasingly prominent

54   in China (Li et al., 2017b; Li et al., 2019b). Therefore, it was critical to accurately reveal the

55   spatiotemporal variation of O_3 pollution and assess its heath risk in China.

56   A growing body of studies began to investigate the spatiotemporal variation of O_3 level

57   worldwide. Wang et al. (2014b) demonstrated that the 8-h O_3 concentration in nearly all of the

58   provincial cities experienced the remarkable increase during 2013-2014. Following the work, Li et

59   al. (2017) reported that the annually mean O_3 concentration over China increased by 9.18% during

60   2014-2016. In other Asian countries except China, Vellingiri et al. (2015) performed long-term

61   obervation and found that the O_3 concentration in Seoul, South Korea displayed gradual increase in

62   the past decades. In the Southeast United States, Li et al. (2018) observed that the surfacee O_3

63   concentration also displayed the gradual decrease in the recent ten years. Although the number of

64   ground-level monitoring sites have been increasing globally, the limited monitoring sites still cannot

65   accurately reflect the fine-scale O_3 pollution status because each site shows small spatial

66   representativeness (0.25-16.25 km^2) (Shi et al., 2018). Furthermore, the number of monitoring

67 sites in many countries (e.g., China and the United States) displays uneven distribution

68 characteristic at the spatial scale. In China, most of these sites focus on North China Plain (NCP)

69 and Yangtze River Delta (YRD), while West China extremely lacks ~~of~~ the ground-level O_3 data,

70 which often increases the uncertainty of health assessment. Therefore, many studies used

71 various models to estimate the O_3 concentration without monitoring sites. Chemical transport

72 models (CTMs) were often considered as the typical methods to predict the surface O_3 level.

73 Zhang et al. (2011) employed the Geos-Chem model to simulate the surface O_3 concentration

74 over the United States, suggesting that the model could capture the spatiotemporal variation of

75 surface O_3 concentration at a large spatial scale. Later on, Wang et al. (2016) developed a hybrid

76 model named land use regression (LUR) coupled with CTMs to predict the surface O_3

77 concentration in the Los Angeles Basin, California. In recent years, these methods were also

78 applied to estimate the surface O_3 level over China. Liu et al. (2018) used Community

79 Multiscale Air Quality (CMAQ) model to simulate the nationwide O_3 concentration over China

80 in 2015. Nonetheless, the high-resolution O_3 prediction using CTMs might be widely deviated

81 from the measured value owing to the imperfect knowledge about the chemical mechanism and

82 the higher uncertainty of emission inventory. Moreover, the continuous emission data of NO_x

83 and VOCs were not always open access, which restricted the long-term estimation of surface

84 O_3 concentration using CTMs.

85 Fortunately, the daily satellite data enable~~s~~ the fine-scale estimation$\underline{s}$ of O_3 level at a

86 regional scale due to broad spatial coverage and high temporal resolution (McPeters et al.,

87 2015). Shen et al. (2019) confirmed that satellite retrieved O_3 column amount can accurately

88 reflect the spatiotemporal distribution of surface O_3 level. Therefore, some studies tried to use

89 traditional statistical models coupled with high-resolution satellite data to estimate the ambient

90 O_3 level. Fioletov et al. (2002) used the satellite measurement to investigate the global

91 distribution of O_3 concentrations based on simple linear model. Recently, Kim et al. (2018)

92 employed the integrated empirical geographic regression method to predict the long-term

93 (1979-2015) variation of ambient O_3 concentration over United States based on O_3 column

94 amount data. Although the statistical modelling of ambient O_3 concentration is widespread all

95 around the world, most of these traditional statistical modelling only utilized the linear model

96 to predict the ambient O_3 concentration, which generally decreased the prediction performance

97 because the nonlinearity and high-order interactions between O_3 and predictors cannot be

98 managed by a simple linear model.

99 As an extension of traditional statistical model, machine learning methods have been widely

100 applied to estimate the pollutant level in recent years because of their excellent predictive

101 performances. Among these machine learning algorithms, decision tree models such as random

102 forest (RF) and extreme gradient boosting (XGBoost) ~~strike a perfect balance between~~

103 ~~prediction performance and computing cost~~generally showed fast training speed and excellent

104 prediction accuracy (Li et al., 2020; Zhan et al., 2018). Furthermore, decision tree models can

105 obtain the contributions of each predictor to air pollutants, which was beneficial to the

106 parameter adaption and model optimization. Chen et al. (2018b) firstly employed RF model to

107 simulate the $PM_{2.5}$ level in China since 2005. Following this work, we recently used the

108 XGBoost model to estimate the 8-h O_3 concentration in Hainan Island for the first time and

109 captured the moderate predictive performance ($R^2 = 0.59$) (Li et al., 2020). While decision tree

110 model shows many advantages in predicting pollutant level, the spatiotemporal autocorrelation

111 of pollutant concentration is not concerned by these studies. Li et al. (2019a) confirmed that the

112 prediction error by decision tree model varied greatly with space and time. Thus, it is imperative

113 to incorporate the spatiotemporal variables into the original model to further improve the

114 performance. To resolve the defects of decision tree models, Zhan et al. (2018) developed a

115 hybrid model named RF-spatiotemporal Kriging (STK) to predict the O_3 concentration over

116 China and achieved the better performance (Overall R^2 = 0.69, Southwest China R^2 = 0.66).

117 Unfortunately, RF-STK model still showed some weaknesses in predicting O_3 concentration.

118 First of all, the predictive performance of the STK model was strongly dependent on the number

119 of monitoring sites and their spatial density. The model often showed worse predictive

120 performance in the region with sparse monitoring sites (Gao et al., 2016). Moreover, the

121 ensemble model cannot simulate the O_3 level during the periods without ground-measured data.

122 In contrast, generalized additive model (GAM) not only considers the time autocorrelation of

123 O_3 concentration, but also shows the better extrapolation ability (Chen et al., 2018a; Ma et al.,

124 2015). Thus, the ensemble model of RF and GAM is proposed to predict the spatiotemporal

125 variation of surface 8-h O_3 concentration.

126   Tibetan Plateau, the highest plateau around the world, shows the higher surface solar

127 radiation compared with the region outside the plateau. It was well documented that high solar

128 radiation ~~is beneficial to~~tended to generate large amount of OH radical, resulting in the O_3

129 formation via the reaction of VOC and OH radical (Ou et al., 2015). While the total O_3 column

130 amount in Tibetan Plateau displayed the slight decrease since 1990s, the convergent airflow

131 formed by subtropical anticyclones could bring ozone-rich air surrounding the plateau to the

132 low atmosphere (Lin et al., 2008), thereby leading to the higher surface O_3 concentration over

133 the plateau. Most studies focused on the stratosphere-troposphere transport of O_3 in Tibetan

134 Plateau, whereas limited effort was spared to investigate ground-level O_3 level over this region.

135 To date, only several studies concerned about the spatiotemporal variation of surface O_3

136 concentration in this region based on field-observation data (Chen et al., 2019; Shen et al., 2014;

137 Yin et al., 2017b). Unfortunately, these scarce monitoring sites in Tibetan Plateau cannot

138 capture real O_3 pollution status especially in the remote areas (e.g., Northern part of Tibetan

139 Plateau) because each site only possessed limited spatial representativeness. Apart from these

140 field measurements, Liu et al. (2018) (R = 0.60) and Zhan et al. (2018) (R^2 = 0.66) used CTM

141 and machine learning model to simulate the surface O_3 concentration over China in 2015,

142 respectively. Both of these studies included the predicted O_3 level in Tibetan Plateau. Although

143 they have finished the pioneering work, the predictive performances of both studies were not

144 very excellent. Therefore, it was imperative to develop a higher quality model to enhance the

145 modelling accuracy.

146 Here, we developed a new hybrid method (RF-GAM) model integrating satellite data,

147 meteorological factors, and geographical variables to simulate the gridded 8-h O_3

148 concentrations over Tibetan Plateau for the first time. Based on the estimated surface O_3

149 concentration, we clarified the long-term variation (2005-2018) of surface O_3 concentration and

150 quantified the key factors for the annual trend. Filling the gap of statistical estimation 8-h O_3

151 level in a remote region, this study provides useful datasets for epidemiological studies and air

152 quality management.

153 **2. Materials and methods**

154 2.1 Study area

带格式的：下标

155   Tibetan Plateau is located in Southwest China ranging from 26.00 to 39.58°N and from

156   73.33 to 104.78°E. Tibetan Plateau is surrounded by Taklamakan Desert to north, Sichuan Basin

157   to southeast. The land area of Tibetan Plateau reaches 2.50 million km^2 (Chan et al., 2006).

158   Based on the air circulation pattern, Tibetan Plateau can be roughly classified into the monsoon-

159   influenced region and the westerly-wind influenced region (Wang et al., 2014a). The annually

160   mean air temperature in most regions are below 0°C. The annually mean rainfall amount in

161   Tibetan Plateau ranges from 50 to 2000 mm. The terrain conditions are complex and the higher

162   altitude focused on the central region. Tibetan Plateau is generally treated as the remote region

163   lack of anthropogenic activity and most of the residents focus on southeast and south parts of

164   Tibetan Plateau. Tibetan Plateau ~~is consisted~~consists of 19 prefecture-level cities and their

165   names and corresponding geographical locations are shown in Fig. 1 and Fig. S1.

166   2.2 Data preparation

167   2.2.1 Ground-level 8-h O_3 concentration

168   The daily 8-h O_3 data in 37 monitoring sites over Tibetan Plateau from May 13th , 2014 to

169   December 31th, 2018 were collected from the national air quality monitoring network. The O_3 levels

170   in all of these sites were determined using an ultraviolet-spectrophotometry method. The highest 8-

171   h moving average O_3 concentration each day was calculated as the daily 8-h O_3 level after data

172   quality assurance. The data quality of all the monitoring sites ~~were~~ was assured on the basis of the

173   HJ 630-2011 specifications. The data with no more than two consecutive hourly measurement

174   missing in each day was treated as the valid data.

175   2.2.2 Satellite-retrieved O_3 column amount

176   The O_3 column amounts (DU) during 2005-2018 were downloaded from the Ozone Monitoring

177 Instrument-O$_3$ (OMI-O$_3$) level-3 data with a 0.25° spatial resolution from the website of National

178 Aeronautics and Space Administration (NASA) (https://www.nasa.gov/). The OMI-O$_3$ product

179 shows global coverage and traverses the earth once a day. The O$_3$ column amount with cloud

180 radiance fraction > 0.5, terrain reflectivity > 30%, and solar zenith angles > 85° should be removed.

181 In addition, the cross-track pixels significantly influenced by row anomaly should be deleted.

182 2.2.3 Meteorological data and geographical covariates

183 The daily meteorological data were obtained from ERA-Interim datasets with 0.125° resolution.

184 These meteorological data were consisted of 2 meter dewpoint temperature (d2m), 2 meter

185 temperature (t2m), 10 meter U wind component (u10), 10 meter V wind component (v10), boundary

186 layer height (blh), sunshine duration (sund), surface pressure (sp), and total precipitation (tp). The

187 30 m-resolution elevation data (DEM) was downloaded from China Resource and Environmental

188 Science Data Center (CRESDC). The data of gross domestic production (GDP) and population

189 density with 1 km resolution were also extracted from CRESDC. Population density and GDP in

190 2005, 2010, and 2015 were integrated into the model to predict the surface 8-h O$_3$ concentration

191 over Tibetan Plateau because these data were available each five years. Additionally, the land use

192 data of 30 m resolution (e.g., waters, grassland, urban, forest) were also extracted from CRESDC.

193 At last, the latitude, longitude, and time were also incorporated into the model.

194 All of the explanatory variables collected were resampled to 0.25° × 0.25° grids to predict the

195 O$_3$ level. The original meteorological data with 0.125° resolution were resampled to 0.25° grid. The

196 land use area, elevation, GDP and population density in each grid were calculated using spatial

197 clipping. Lastly, all of the predictors were integrated into an intact table to train the model.

198 2.3 Model development and assessment

199   The RF-GAM model was regarded as the hybrid model of RF and GAM. The RF-GAM model

200   is a two-stage model that the prediction error estimated by the RF model was then simulated by

201   GAM. The prediction results of RF and GAM were summed as the final result of RF-GAM model

202   (Fig. 2). The detailed equation is as follows:

203     $$Z(s,t) = P(s,t) + E(s,t) \qquad (1)$$

204   where $Z(s,t)$ is the estimated 8-h O_3 level at the location s and time t; $P(s,t)$ represents the 8-h O_3

205   concentration predicted by the RF model; $E(s,t)$ denotes the prediction error by GAM.

206   In the RF model, a large number of decision trees were planted based on the bootstrap sampling

207   method. At each node of the decision tree, a random sample of all predictors was applied to

208   determine the best split among them. Following the procedure, a simple majority vote was employed

209   to predict the 8-h O_3 level. The RF model avoided priori linear assumption of O_3 concentration and

210   predictors, which was often not in good agreement with actual state. The RF model has two key

211   parameters including n_{tree} (the number of trees grown) and m_{try} (the number of explanatory variables

212   sampled for splitting at each node). The prediction performance of the RF model was strongly

213   dependent on the two parameters. The optimal n_{tree} and m_{try} were determined based on the least out-

214   of-bag (OOB) errors. Based on the iteration result, the optimal n_{tree} and m_{try} reached 500 and 5,

215   respectively. Besides, the backward variable selection method was performed on the RF submodel

216   to achieve the better performance. At each step of the predictor selection, the variable with the least

217   important value was excluded from the next step. This one-variable-at-a-time exclusion method was

218   repeated until only two explanatory variables remained in the submodel. Finally, all of the selected

219   variables except the area of waters were integrated into the model to achieve the best prediction

220   performance. The detailed RF model is as follows:

221

$$O_3 = O_3 \; column + Elevation + Agr + Urban + Forest + GDP + Grassland + Population + \Pr ec + T + WS + P + tsun + RH \quad (2)$$

222 where O_3 denotes the observed 8-h O_3 level in the monitoring site; the O_3 column represents the O_3

223 column amount in the corresponding grid; Elevation denotes the corresponding elevation of the site;

224 Agr, Urban, Forest, Grassland are the agricultural land, urban land, forest land, and the grassland,

225 respectively. Population represents the population density in the corresponding site. Prec, T, WS, P,

226 tsun, and RH are precipitation, air temperature, wind speed, air pressure, sunshine duration, and

227 relative humidity, respectively. Additionally, other five models including RF, generalized regression

228 neutral network (GRNN), backward propagation neural network (BPNN), Elman neural network

229 (ElmanNN), and extreme learning machine (ELM) also used the backward variable selection

230 method. The R^2 value was treated as an important parameter to add or reduce the variable. The

231 variable should be removed when the R^2 value of the submodel showed the remarkable decrease

232 with the integration of this variable. Lastly, the optimal variable group was applied to establish the

233 submodel.

234 Following the RF submodel, the prediction error estimated by the RF submodel was further

235 modelled by the GAM. GAM could reflect the time autocorrelation of predictive error of RF model,

236 and thus the ensemble model of RF and GAM might decrease the modelling error of one-stage

237 model. All of the variables were incorporated into the models to establish the second-stage model,

238 and the backward variable selection was also used to determine the optimal variable group.

239 The 10-fold cross-validation (CV) technique was employed to evaluate the predictive

240 performances for all of the machine learning models. All of the training data set were randomly

241 classified into 10 subsets uniformly. In each round of validation, nine subsets were used to train and

242 the remaining subset was applied to test the model performance. The process was repeated 10 times

243 until every subset has been tested. Some statistical indicators including R^2, Root Mean Square Error

244 (RMSE), Mean Prediction Error (MPE) and the slope were calculated to assess the model

245 performance. The optimal model with the best performance was used to estimate the 8-h O_3

246 concentration in the past decades.

247 **3. Results and discussion**

248 3.1 The validation of model performance

249 Figure 3 and figure S2 show the density scatterplots of the fitting and 10-fold cross-validation

250 results for eight machine learning models for China. The 10-fold cross-validation R^2 values

251 followed the order of RF-GAM ($R^2 = 0.76$) > RF-STK ($R^2 = 0.63$) > RF ($R^2 = 0.55$) > GRNN ($R^2 =$

252 0.53) > BPNN ($R^2 = 0.50$) > XGBoost ($R^2 = 0.48$) > ElmanNN ($R^2 = 0.47$) > ELM ($R^2 = 0.32$). The

253 RMSE values of RF-GAM, RF-STK, RF, GRNN, XGBoost, BPNN, ElmanNN, and ELM were

254 14.41, 17.79, 19.13, 19.41, 20.73, 20.06, 20.61, and 23.36 μg/m³, respectively. Both of MPE and

255 RPE showed the similar characteristic with RMSE in the order of RF-GAM (10.97 μg/m³ and

256 26.50%) < RF-STK (13.48 μg/m³ and 35.15%) < RF (14.71 μg/m³ and 35.51%) < GRNN (14.89

257 μg/m³ and 35.82%) < BPNN (15.43 μg/m³ and 36.19%) < ElmanNN (15.75 μg/m³ and 37.05%) <

258 XGBoost (15.80 μg/m³ and 38.13%) < ELM (18.23 μg/m³ and 44.05%) (Fig. 3 and Fig. S2). Besides,

259 the slope of the RF-GAM model was closer to 1 compared with other models. It was well

260 documented that the RF model generally showed the better performance than other models because

261 this method did not need to define complex relationships between the explanatory variables and the

262 O_3 concentration (e.g., linear or nonlinear). Furthermore, the variable importance indicators

263 calculated by the RF model can help user to distinguish the key variables from noise ones and make

264 full use of the strength of each predictor to assure the model robustness. Although BPNN, GRNN,

265 XGBoost, ElmanNN, and ELM have been widely applied to estimate the air pollutant concentrations

266 (Chen et al., 2018c; Zang et al., 2018; Zhu et al., 2019), these methods suffered from some

267 weaknesses in predicting the pollutant level. For instance, both of BPNN and ElmanNN models

268 could capture the locally optimal solution when the training subsets were integrated into the final

269 model, which decreased the predictive performance of the model (Wang et al., 2015). Moreover,

270 BPNN generally showed slow training speed, especially with the huge training subsets (Li and Park,

271 2009; Wang et al., 2015). ELM often consumed more computing resource and experienced the over-

272 fitting issue due to the increase of sampling size (Huang et al., 2015; Shao et al., 2015). GRNN

273 method advanced the training speed compared with BPNN model and avoided the locally optimal

274 solution during the modelling process (Zang et al., 2019), whereas the predictive performance is

275 still worse than that of RF model. XGBoost was often considered to be robust in predicting air

276 pollutant level (Li et al., 2020), while the model did not display the excellent performance in the

277 present study. It might be attributable to that the sampling size in the present study was not enough

278 because the model generally showed the better performance with big samples. Moreover, we found

279 that the two-stage model was superior to the one-way model in the predictive performance. The

280 encouraging result suggested that the relationship between the predictors and the 8-h O_3

281 concentration varied with space and time. The two-stage model used the GAM method to further

282 adjust the prediction error of the RF model, and considered the spatiotemporal correlation of

283 predictor error in Tibetan Plateau. Although the STK model incorporated space and time into the

284 model simultaneously, the RF-GAM model outperformed the RF-STK model. It was assumed that

285 the STK model showed the higher uncertainty in predicting the O_3 concentration in the region with

286 scarce sampling sites (Gao et al., 2016; Li et al., 2017a). Overall, the ensemble RF-GAM model

287 showed the significant improvement in predictive performance.

288 The performances of RF-GAM displayed slight difference in each year during 2014-2018. As

289 shown in Table 1, the R^2 value showed the highest value (0.76) in 2016, followed by that in 2018

290 (0.75), 2017 (0.73), 2015 (0.72), and the lowest one in 2014 (0.69). Both of RMSE and MPE

291 exhibited the lowest values in 2014, while these parameters did not show significant variation during

292 2015-2018. The lowest R^2 value and the highest RPE focused on 2014 due to the least sample size,

293 while the highest R^2 value and lowest RPE in 2016 was contributed by the maximum sample size.

294 Geng et al. (2018) found that the predictive performance of machine learning model was strongly

295 dependent on the number of training samples and sampling frequency. The lower RMSE and MPE

296 in 2014 might be attributable to the lack of measured O_3 data in spring, which decreased the higher

297 value of O_3 concentration. The performances of the RF-GAM model in four seasons were also

298 assessed by 10-fold cross-validation (Table 2). The predictive performance of the RF-GAM model

299 showed significantly seasonal difference with the highest R^2 value observed in summer (0.74),

300 followed by winter (0.69) and autumn (0.67), and the lowest one in spring (0.64). However, both of

301 RMSE and MPE displayed different seasonal characteristics with the R^2 value. Both of RMSE and

302 MPE for RF-GAM followed the order of spring (15.32 and 11.94 μg/m^3) > summer (15.13 and 11.75

303 μg/m^3) > winter (14.58 and 11.44 μg/m^3) > autumn (13.23 and 10.52 μg/m^3). The lowest R^2 value

304 in spring might be caused by multiple O_3 sources and complicate O_3 formation mechanisms. On the

305 one hand, the O_3 in spring might be generated from the local anthropogenic emission or long-range

306 transport (Li et al., 2017; Li et al., 2019b). On the other hand, a strong stratosphere-troposphere

307 exchange process due to lower height of troposphere in Tibetan Plateau might lead to the higher O_3

308 concentration in spring (Skerlak et al., 2014). Unfortunately, both of long-range transport and

309 stratosphere-troposphere exchange process were missing in the RF-GAM model, which restricted

310 the accuracy of O$_3$ estimation in spring. The large estimation errors (e.g., RMSE and , MPE, and

311 RPE) in spring and summer were attributable to the high 8-h O$_3$ concentration in these seasons,

312 while the low prediction error observed in autumn was contributed by the low O$_3$ level.

313 Apart from the seasonal variation, we also investigated the spatial variability variabilities of the

314 predictive accuracy for RF-GAM model. Tibetan Plateau was classified into five provinces and then

315 the predictive performance of RF-GAM model in each province was calculated. Among the five

316 provinces, Gansu province displayed the highest R^2 value (0.74), followed by Sichuan province

317 (0.71), Qinghai province (0.70), Tibet autonomous region (0.69), and Yunnan province (0.54) (Table

318 3). The result shown herein was not in agreement with the previous studies by Geng et al. (2018),

319 who confirmed that the predictive performance of machine learning model was positively associated

320 with the sampling size. It was assumed that the spatial distribution of the sampling sites in Tibet was

321 uneven and the sampling density is low, though Tibet possessed the maximum monitoring sites

322 compared with other provinces. The prediction error (RMSE and MPE) did not exhibit the same

323 characteristics with the R^2 value. The higher RMSE and MPE focused on Tibet autonomous region

324 (14.81 and 11.24 μg/m^3) and Qinghai province (14.83 and 11.33 μg/m^3) due to the higher values of

325 blh and sund. The lowest values of RMSE and MPE could be observed in Yunnan province, which

326 was contributed by the higher rainfall amount. The highest RPE was concentrated on Yunnan

327 province (25.85%), followed by Tibet (22.90%), Qinghai (22.65%), Sichuan (22.62%), and the

328 lowest one in Gansu province (22.51%), which might be linked with the sample size.

329 Although 10-fold cross-validation verified that the RF-GAM model showed the better predictive

330 performance in estimating the surface 8-h O$_3$ concentration, the test method cannot validate the

331 transferring ability of the final model. The monitoring site in Tibetan Plateau before May, 2014 is

332 very limited, and only the daily 8-h O_3 data in Lhasa from the open website

333 (https://www.aqistudy.cn/historydata/) was available to compare with the simulated data. As

334 depicted in Fig. 4, the R^2 value of unlearning 8-h O_3 level against predicted 8-h O_3 concentration

335 reached 0.67, which was slightly lower than that of the 10-fold cross-validation R^2 value. Overall,

336 the extrapolation ability of the RF-GAM model is satisfactory, and thus it was supposed that the

337 model could be applied to estimate the O_3 concentration in other years. Both of RMSE and MPE

338 for the unlearning 8-h O_3 level against the predicted 8-h O_3 concentration were significantly higher

339 than those of the 10-fold cross-validation. It was supposed that Lhasa showed the higher surface 8-

340 h O_3 concentration over Tibetan Plateau.

341 To date, some previous studies also simulated the surface O_3 concentration in Tibetan Plateau

342 using statistical models (Zhan et al., 2018). For instance, Zhan et al. (2018) employed the RF-STK

343 model to estimate the surface O_3 concentration over China, and explained the 66% spatial variability

344 of O_3 level in Tibetan Plateau. Apart from these statistical models, some classical CTMs were also

345 applied to estimate the O_3 concentration in the remote area. Both of Liu et al. (2018) and Lin et al.

346 (2018) used CMAQ to estimate the O_3 level across China, while the R^2 values in most of cities were

347 lower than 0.50. In terms of the predictive performance, the RF-GAM model in our study showed

348 the significant advantages compared with previous studies. It should be noted that our RF-GAM

349 model could outperform most of current models, chiefly because of (1) accounting for the temporal

350 autocorrelation of surface O_3 concentration; and (2) the use of high-quality satellite data.

351 3.2 Variable importance

352 The results of variable importance for key variables are depicted in Fig. 5. In the final RF-GAM

353 model, it was found that time was the dominant factor for the 8-h O_3 concentration in Tibetan Plateau,

354 indicating that the ambient O_3 concentration displayed significantly temporal correlation. Following

355 the time, meteorological factors served as the main factors for the O_3 pollution in the remote region.

356 The sum of sund, sp, d2m, t2m, and tp occupied 34.43% of the overall variable importance. Among

357 others, sund was considered to be the most important meteorological factors for the O_3 pollution. It

358 was assumed that strong solar radiation and long duration of sunshine favored the photochemical

359 generation of ambient O_3 (Malik and Tauler, 2015; Stähle et al., 2018). Tan et al. (2018)

360 demonstrated that the chemical reaction between NO_x and VOCs was strongly dependent on the

361 sunlight. Besides, the atmospheric pressure (sp) was also treated as a major driver for the O_3

362 pollution over Tibetan Plateau. Santurtún et al. (2015) have demonstrated that sp was closely linked

363 to the atmospheric circulation and synoptic scale meteorological pattern, which could influence the

364 long-range transport of ambient O_3. Apart from sund and sp, d2m and t2m played significant role

365 on the O_3 pollution, which was in consistent with many previous studies (Zhan et al., 2018). Zhan

366 et al. (2018) observed that cold temperature was not favorable to the O_3 formation. d2m can affect

367 the surface O_3 pollution through two aspects. On the one hand, RH affected heterogeneous reactions

368 of O_3 and particles (e.g., soot, mineral) (He et al., 2017; He and Zhang, 2019; Yu, 2019). On the

369 other hand, high RH could increase the soil moisture and evaporation, and thus the water-stressed

370 plants tended to emit more biogenic isoprene, thereby promoting the elevation of O_3 concentration

371 (Zhang and Wang, 2016). It should be noted that the effect of precipitation on O_3 pollution was

372 relatively weaker than those of other meteorological factors. Zhan et al. (2018) also found the similar

373 result and believed that rain scavenging served as the key pathway for the O_3 removal only when

374 O_3 pollution was very serious. The power of O_3 column amount on surface O_3 concentration seemed

375 to be lower than those of most meteorological factors, suggesting that vertical transport of ambient

376 O$_3$ was complex. Although socioeconomic factors and land use types were not dominant factors for

377 the O$_3$ pollution in Tibetan Plateau, they still cannot be ignored in the present study because the

378 predictive performance would worsen if these variables were excluded from the model. It was

379 widely acknowledged that the anthropogenic emissions ~~of NO$_x$ and VOCs~~ focused on the developed

380 urban areas with high population density especially in the remote plateau (Zhang et al., 2007; Zheng

381 et al., 2017). Compared with the urban land, the grassland played more important role on the O$_3$

382 pollution in Tibetan Plateau. It was thus supposed that the grassland was widely distributed on

383 Tibetan Plateau, which could release a large amount of biogenic volatile organic compounds

384 (BVOCs) (Fang et al., 2015). It was well known that photochemical reactions of BVOCs and NO$_x$

385 in the presence of sunlight caused ~~was beneficial to~~ the O$_3$ formation (Calfapietra et al., 2013; Yu et

386 al., 2006). Furthermore, Fang et al. (2015) confirmed that the BVOC emission in Tibetan Plateau

387 displayed a remarkable increase in the wet seasons.

388 3.3 The spatial distribution of estimated 8-h O$_3$ concentration over Tibetan Plateau

389   Figure 6 depicts the spatial distribution of the 8-h O$_3$ level estimated by the novel RF-GAM

390 model. The spatial distribution pattern modelled by the RF-GAM model showed the similar

391 characteristic with the result simulated by previous studies except North Tibetan Plateau (Liu et al.,

392 2018). The estimated 8-h O$_3$ concentration displayed the highest value in some cities of North

393 Tibetan Plateau such as Huangnan (73.48±4.53 μg/m^3) and Hainan (72.24±5.34 μg/m^3), followed

394 by the cities in the central region including Lhasa (65.99±7.24 μg/m^3) and Shigatse (65.15±6.14

395 μg/m^3), and the lowest one in some cities of Southeast Tibetan Plateau such as Aba (55.17±12.77

396 μg/m^3). The spatial pattern of 8-h O$_3$ concentration is highly consistent with the result predicted by

397 Liu et al. (2018) using CMAQ model, while it is not in agreement with the result estimated by Zhan

398 et al. (2018) using RF-STK model. The difference of the present study and Zhan et al. (2018) focuses

399 on the North Tibetan Plateau, which lacks of monitoring site and remains the higher uncertainty.

400 Firstly, it might be contributed by the weakness of RF-STK mentioned above. Moreover, Zhan et al.

401 (2018) only used the ground-level measured data in 2015 to establish the model and the data in new

402 sites since 2015 were not incorporated into the model, which could increase the model uncertainty

403 (Zhan et al., 2018). As shown in Fig. 6, most of the cities in Qinghai province (e.g., Huangnan,

404 Hainan, and Guoluo) generally showed the higher 8-h O_3 concentration over Tibetan Plateau, which

405 was in a good agreement with the spatial distribution of O_3 column amount (Fig. S3). Besides, some

406 cities in Tibet such as Shigatse and Lhasa also showed the higher 8-h O_3 levels. It was supposed that

407 the precursor (e.g., NO_x and $VOCs$) emissions in these regions were significantly higher than those

408 in other cities of Tibetan Plateau (Fig. S4). Zhang et al. (2007) used the satellite data to observe that

409 the higher VOCs and NO_x emission focused on the residential area with high population density in

410 the remote Tibetan Plateau. Apart from the effect of anthropogenic emission, the meteorological

411 conditions could be also the important factors for the 8-h O_3 concentration. As shown in Fig. S5-

412 S10, the higher blh and sp in the Northeast Tibetan Plateau were beneficial tomight promote the O_3

413 formation through the reaction of VOC and OH radical, leading to the higher 8-h O_3 concentration

414 in these cities (Ou et al., 2015). In addition, the lower tp occurred in North Tibetan Plateau and

415 Northeast Tibetan Plateau, both of which were unfavorable to the ambient O_3 removal (Yoo et al.,

416 2014). In contrast, the higher tp observed in the Southeast Tibetan Plateau resulted in the slight O_3

417 pollution.

418 3.4 The temporal variation of the simulated 8-h O_3 concentration over Tibetan Plateau

419   The annually mean estimated 8-h O_3 concentration in Tibetan Plateau displayed the slow

420   increase from 64.74 ± 8.30 μg/m^3 to 66.45 ± 8.67 μg/m^3 2005 through 2015 (Table S1), whereas it

421   decreased from the peak to 65.87 ± 8.52 μg/m^3 during 2015-2018 (Fig. 7). Based on the Mann-

422   Kendall method (Fig. 8a), it was found that the surface O_3 concentration exhibited the slight increase

423   as the whole, while the increase degree was not significant ($p > 0.05$). Besides, it should be noted

424   that the O_3 concentrations in various regions showed different increase speed. As depicted in Fig.

425   8b, we found that the 8-h O_3 concentrations in North, West, and East Tibetan Plateau displayed

426   significant increase trend by the speed of 1-3 μg/m^3 during 2005-2018. The middle region of Tibetan

427   Plateau showed the moderate increase trend by the speed of 0-1 μg/m^3. However, the 8-h O_3

428   concentration in Shigatse and Sannan even displayed the decrease trend 2005 through 2018.

429   Besides, the 8-h O_3 concentrations in Tibetan Plateau displayed significantly seasonal

430   discrepancy. The estimated 8-h O_3 level in Tibetan Plateau followed the order of spring (75.00 ± 8.56

431   μg/m^3) > summer (71.05 ± 11.13 μg/m^3) > winter (56.39 ± 7.42 μg/m^3) > autumn (56.13 ± 8.27 μg/m^3)

432   (Fig. 9 and Table 4). The 8-h O_3 concentrations in most of prefecture-level cities showed the

433   similarly seasonal characteristics with the overall seasonal variation in Tibetan Plateau. Based on

434   the result summarized in Table S2, it was found that the key precursors of ambient O_3 generally

435   displayed the higher emissions in winter compared with other seasons. However, the seasonal

436   distribution of ambient O_3 concentration was not in accordance with the precursor emissions,

437   suggesting that the meteorological factors might play more important roles on ambient O_3

438   concentration. It was well known that the higher air temperature in spring and summer was were

439   closely related to the low sp and high sund, both of which were beneficial to thepromoted O_3

440   formation (Sitnov et al., 2017). Although summer showed the highest air temperature and the longest

441   sunshine duration, the higher rainfall amount in summer decreased the ambient O_3 concentration

442 via wet deposition (Li et al., 2017b; Li et al., 2019b). Moreover, the highest blh occurred in spring,

443 which was favorable to the strong stratosphere-troposphere exchange process in Tibetan Plateau

444 (Skerlak et al., 2014). Therefore, the 8-h O_3 concentration in summer and winter were relatively

445 lower than that in spring. Nonetheless, the 8-h O_3 levels in Diqing, Sannan, and Nyingchi displayed

446 the highest values in spring (56.38±7.87, 73.90±5.97, and 73.22±2.77 μg/m^3), followed by winter

447 (45.88±7.05, 61.71±4.32, and 62.24±3.63 μg/m^3) and summer (44.35±5.90, 61.00±5.86, and

448 59.60±2.33 μg/m^3), and the lowest ones in autumn (37.45±5.76, 54.70±3.13, and 53.84±2.06 μg/m^3).

449 The lower O_3 level in summer than winter was mainly attributable to the higher precipitation

450 observed in the summer of these cities (Fig. S11). In addition, it should be noted that the NO_x and

451 VOCs emissions of South Tibetan Plateau (e.g., Sannan) exhibited the higher values in winter

452 compared with other seasons.

453 3.5 The nonattainment days over Tibetan Plateau during 2005-2018

454 The annually mean nonattainment days in the 19 prefecture-level cities over Tibetan Plateau are

455 summarized in Table 2. 100 μg/m^3 was regarded as the critical value for the 8-h O_3 level by World

456 Health Organization (WHO). The nonattainment days denoted total days with the 8-h O_3

457 concentration higher than 100 μg/m^3. Although the annually mean 8-h O_3 concentrations in all of

458 the cities over Tibetan Plateau did not exceed the critical value, not all of the regions experienced

459 excellent air quality in the long period (2005-2018). Some cities of Qinghai province including

460 Huangnan, Haidong, and Guoluo suffered from 45, 40, and 40 nonattainment days each year (Fig.

461 10 and Table 5). Besides, some cities in the South Tibetan Plateau such as Shigatse and Sannan also

462 experienced more than 40 nonattainment days each year, suggesting that Tibetan Plateau was still

463 faced of the risk for O_3 pollution. Fortunately, some remote cities such as Ali, Ngari, and Qamdo

464 did not experience the excessive O_3 pollution all the time, which was ascribed to the low precursor

465 emissions and appropriate meteorological conditions. It should be noted that the nonattainment days

466 in the region with high O_3 concentration showed the significantly seasonal difference, whereas the

467 seasonal difference was not remarkable in the city with low O_3 pollution. As shown in Table 2, it

468 should be noted that nearly all of the nonattainment days could be detected in spring and summer,

469 which was in good agreement with the O_3 levels in different seasons, indicating that the O_3 pollution

470 issue should be paid more attention in spring and summer.

471   The determination of nonattainment days showed some uncertainties owing to the predictive

472 error of modelled O_3 concentration. First of all, meteorological data used in RF-GAM model were

473 collected from reanalysis data and these gridded data often showed some uncertainties, which could

474 increase the uncertainty of O_3 estimation. Second, the O_3 column amount used in the present study

475 reflected vertical O_3 column amount rather than surface O_3 concentration. Thus, it could decrease

476 the predictive performance of surface O_3 level.

477 **4. Summary and implication**

478   In the present study, we developed a novel hybrid model (RF-GAM) based on multiple

479 explanatory variables to estimate the surface 8-h O_3 concentration across the remote Tibetan Plateau.

480 The 10-fold cross-validation method demonstrated that RF-GAM achieved excellent performance

481 with the highest R^2 value (0.76) and lowest root mean square error (RMSE) (14.41 μg/m^3) compared

482 with other model including RF-STK, RF, BPNN, XGBoost, GRNN, ElmanNN, and ELM models.

483 Moreover, the unlearning ground-measured O_3 data validated that the RF-GAM model showed the

484 better extrapolation performance (R^2=0.67, RMSE=25.68 μg/m^3). The result of variable importance

485 suggested that time, sund, and sp were key factors for the surface 8-h O_3 concentration over Tibetan

486 Plateau. Based on the RF-GAM model, we found that the estimated 8-h O_3 concentration exhibited

487 notably spatial variation with the highest value in some cities of North Tibetan Plateau such as

488 Huangnan (73.48±4.53 μg/m³) and Hainan (72.24±5.34 μg/m³) and the lowest one in some cities of

489 Southeast Tibetan Plateau such as Aba (55.17±12.77 μg/m³). Besides, we also found that the O_3

490 level displayed a slow increase from 64.74±8.30 μg/m³ to 66.45±8.67 μg/m³ 2005 through 2015,

491 while the O_3 concentration decreased to 65.87±8.52 μg/m³ in 2018. The estimated 8-h O_3 level in

492 Tibetan Plateau showed the significantly seasonal discrepancy with the order of spring (75.00±8.56

493 μg/m³) > summer (71.05±11.13 μg/m³) > winter (56.39±7.42 μg/m³) > autumn (56.13±8.27 μg/m³).

494 Based on the critical value set by WHO, most of the cities in Tibetan Plateau shared with the

495 excellent air quality, while several cities (e.g., Huangnan, Haidong, and Guoluo) still suffered from

496 more than 40 nonattainment days each year.

497 The RF-GAM model for O_3 estimation has several limitations. First of all, the O_3 estimation in

498 North Tibetan Plateau might show some uncertainties because the ground-level monitoring site is

499 very scarce, and thus we cannot validate the reliability of predicted value in the region without

500 monitoring site. Secondly, our approach did not include data on emission inventory, or traffic count

501 because the continuous emissions of NO_x and VOCs were not open access. At last, we only focused

502 on the temporal variation of surface O_3 concentration in recent ten years, and the short-term O_3 data

503 cannot reflect the response of O_3 pollution to climate change. In the future work, we should combine

504 more explanatory variables such as long-term NO_x and VOCs emissions to retrieve the surface O_3

505 level over Tibetan Plateau in the past decades.

506 **Author contributions**

507 This study was conceived by Rui Li and Hongbo Fu. Statistical modelling was performed by Rui

508   Li, Yilong Zhao, Ya Meng, Wenhui Zhou and Ziyu Zhang. Rui Li drafted the paper.

509   **Acknowledgements**

510   This work was supported by National Natural Science Foundation of China (Nos. 91744205,

511   21777025, 21577022, 21177026).

512   **Reference**

513   Bornman, J.F., Barnes, P.W., Robson, T.M., Robinson, S.A., Jansen, M.A., Ballaré, C.L., Flint, S.D.:

514   Linkages between stratospheric ozone, UV radiation and climate change and their implications for

515   terrestrial ecosystems. Photoch. Photobio. Sci. 18, 681-716, 10.1039/C8PP90061B, 2019.

516   Calfapietra, C., Fares, S., Manes, F., Morani, A., Sgrigna, G., Loreto, F.: Role of Biogenic Volatile

517   Organic Compounds (BVOC) emitted by urban trees on ozone concentration in cities: A review.

518   Environ. Pollut. 183, 71-80, https://doi.org/10.1016/j.envpol.2013.03.012, 2013.

519   Chan, C., Wong, K., Li, Y., Chan, L., Zheng, X.: The effects of Southeast Asia fire activities on

520   tropospheric ozone, trace gases and aerosols at a remote site over the Tibetan Plateau of Southwest

521   China. Tellus B 58, 310-318, https://doi.org/10.1111/j.1600-0889.2006.00187.x, 2006.

522   Chen, G., Knibbs, L.D., Zhang, W., Li, S., Cao, W., Guo, J., Ren, H., Wang, B., Wang, H., Williams, G.:

523   Estimating spatiotemporal distribution of PM_1 concentrations in China with satellite remote sensing,

524   meteorology, and land use information. Environ. Pollut. 233, 1086-1094,

525   https://doi.org/10.1016/j.envpol.2017.10.011, 2018a.

526   Chen, G., Li, S., Knibbs, L.D., Hamm, N., Cao, W., Li, T., Guo, J., Ren, H., Abramson, M.J., Guo, Y.: A

527   machine learning method to estimate $PM_{2.5}$ concentrations across China with remote sensing,

528   meteorological and land use information. Sci. Total Environ. 636, 52-60,

529   https://doi.org/10.1016/j.scitotenv.2018.04.251, 2018b.

530   Chen, G., Morawska, L., Zhang, W., Li, S., Cao, W., Ren, H., Wang, B., Wang, H., Knibbs, L.D., Williams,

531   G.: Spatiotemporal variation of PM_1 pollution in China. Atmos. Environ. 178, 198-205,

532   https://doi.org/10.1016/j.atmosenv.2018.01.053, 2018c.

533   Chen, P., Yang, J., Pu, T., Li, C., Guo, J., Tripathee, L., Kang, S.: Spatial and temporal variations of

534   gaseous and particulate pollutants in six sites in Tibet, China, during 2016-2017. Aerosol Air Qual.

535   Res. 19, 516-527, doi: 10.4209/aaqr.2018.10.0360, 2019.

536   Emberson, L.: Critical air quality effects: A focus on assessing crop growth, productivity and socio-

537   economic implications of food supply. Air Qual. Climat. Change 51, 50, 2017.

538   Fang, K., Makkonen, R., Guo, Z., Zhao, Y., Seppä, H.: An increase in the biogenic aerosol concentration

539   as a contributing factor to the recent wetting trend in Tibetan Plateau. Sci. Rep. 5, 14628, doi:

540   10.1038/srep14628, 2015.

541   Feng, Z., De Marco, A., Anav, A., Gualtieri, M., Sicard, P., Tian, H., Fornasier, F., Tao, F., Guo, A.,

542   Paoletti, E.: Economic losses due to ozone impacts on human health, forest productivity and crop

543   yield across China. Environ. Interna. 131, 104966, https://doi.org/10.1016/j.envint.2019.104966,

544   2019.

545   Feng, Z., Hu, E., Wang, X., Jiang, L., Liu, X.: Ground-level O_3 pollution and its impacts on food crops

546   in China: a review. Environ. Pollut. 199, 42-48, https://doi.org/10.1016/j.envpol.2015.01.016, 2015.

547   Fioletov, V., Bodeker, G., Miller, A., McPeters, R., Stolarski, R.: Global and zonal total ozone variations

548   estimated from ground-based and satellite measurements: 1964-2000. J. Geophy. Res. 107, ACH 21-

549   21-ACH 21-14, https://doi.org/10.1029/2001JD001350, 2002.

550   Fu, Y., Liao, H., Yang, Y.: Interannual and decadal changes in tropospheric ozone in China and the

551   associated   chemistry-climate   interactions: A   review.   Adv.   Atmos.   Sci.   36,   975-993,

552 https://doi.org/10.1007/s00376-019-8216-9, 2019.

553 Gao, Z., Shao, X., Jiang, P., Cao, L., Zhou, Q., Yue, C., Liu, Y., Wang, C.: Parameters optimization of

554 hybrid fiber laser-arc butt welding on 316L stainless steel using Kriging model and GA. Optics &

555 Laser Technology 83, 153-162, https://doi.org/10.1016/j.optlastec.2016.04.001, 2016.

556 Geng, G., Murray, N.L., Chang, H.H., Liu, Y.: The sensitivity of satellite-based $PM_{2.5}$ estimates to its

557 inputs: Implications to model development in data-poor regions. Environ. Interna.121, 550-560,

558 https://doi.org/10.1016/j.envint.2018.09.051, 2018.

559 Ghude, S.D., Chate, D., Jena, C., Beig, G., Kumar, R., Barth, M., Pfister, G., Fadnavis, S., Pithani, P.:

560 Premature mortality in India due to $PM_{2.5}$ and ozone exposure. Geophy. Res. Lett. 43, 4650-4658,

561 https://doi.org/10.1002/2016GL068949, 2016.

562 He, X., Pang, S., Ma, J., Zhang, Y.: Influence of relative humidity on heterogeneous reactions of O_3 and

563 O_3/SO_2 with soot particles: potential for environmental and health effects. Atmos. Environ. 165, 198-

564 206, https://doi.org/10.1016/j.atmosenv.2017.06.049, 2017.

565 He, X., Zhang, Y.-H.: Influence of relative humidity on SO_2 oxidation by O_3 and NO_2 on the surface of

566 TiO_2 particles: Potential for formation of secondary sulfate aerosol. Spectrochimica Acta Part A:

567 Molecular and Biomolecular Spectroscopy 219, 121-128, https://doi.org/10.1016/j.saa.2019.04.046,

568 2019.

569 Huang, G., Huang, G.-B., Song, S., You, K.: Trends in extreme learning machines: A review. Neural

570 Networks 61, 32-48, https://doi.org/10.1016/j.neunet.2014.10.001, 2015.

571 Kim, S.-Y., Bechle, M., Hankey, S., Sheppard, E.L.A., Szpiro, A.A., Marshall, J.D.: Concentrations of

572 criteria pollutants in the contiguous US, 1979–2015: Role of model parsimony in integrated empirical

573 geographic regression, 2018.

574   Li, C.H., Park, S.C.: Combination of modified BPNN algorithms and an efficient feature selection

575   method for text categorization. Inform. Process Manag. 45, 329-340,

576   https://doi.org/10.1016/j.ipm.2008.09.004, 2009.

577   Li, H., Liu, T., Wang, M., Zhao, D., Qiao, A., Wang, X., Gu, J., Li, Z., Zhu, B.: Design optimization of

578   stent and its dilatation balloon using kriging surrogate model. Biomed. Eng. Online 16, 13, 2017a.

579   Li, J.Y., Mao, J.Q., Fiore, A.M., Cohen, R.C., Crounse, J.D., Teng, A.P., Wennberg, P.O., Lee, B.H.,

580   Lopez-Hilfiker, F.D., Thornton, J.A., Peischl, J., Pollack, I.B., Ryerson, T.B., Veres, P., Roberts, J.M.,

581   Neuman, J.A., Nowak, J.B., Wolfe, G.B., Horowitz, L.W.: Decadal changes in summertime reactive

582   oxidized nitrogen and surface ozone over the Southeast United States. Atmos. Chem. Phys. 18, 2341–

583   2361, https://doi.org/10.5194/acp-18-2341-2018, 2018.

584   Li, R., Cui, L., Li, J., Zhao, A., Fu, H., Wu, Y., Zhang, L., Kong, L., Chen, J.: Spatial and temporal

585   variation of particulate matter and gaseous pollutants in China during 2014–2016. Atmos. Environ.

586   161, 235-246, https://doi.org/10.1016/j.atmosenv.2017.05.008, 2017b.

587   Li, R., Cui, L., Meng, Y., Zhao, Y., Fu, H.: Satellite-based prediction of daily SO_2 exposure across China

588   using a high-quality random forest-spatiotemporal Kriging (RF-STK) model for health risk

589   assessment. Atmos. Environ. 208, 10-19, https://doi.org/10.1016/j.atmosenv.2019.03.029, 2019a.

590   Li, R., Wang, Z., Cui, L., Fu, H., Zhang, L., Kong, L., Chen, W., Chen, J.: Air pollution characteristics

591   in China during 2015–2016: Spatiotemporal variations and key meteorological factors. Sci. Total

592   Environ. 648, 902-915, https://doi.org/10.1016/j.scitotenv.2018.08.181, 2019b.

593   Li, R., Cui, L.L, Fu, H.B., Li, J.L., Zhao, Y.L., Chen, J.M.: Satellite-based estimation of full-coverage

594   ozone (O_3) concentration and health effect assessment across Hainan Island. J. Clean Prod. 118773,

595   https://doi.org/10.1016/j.jclepro.2019.118773, 2020.

596 Lin, W., Zhu, T., Song, Y., Zou, H., Tang, M., Tang, X., Hu, J.: Photolysis of surface O_3 and production

597   potential of OH radicals in the atmosphere over the Tibetan Plateau. J. Geophy. Res. 113,

598   https://doi.org/10.1029/2007JD008831, 2008.

599 Lin, Y.Y., Jiang, F., Zhao, J., Zhu, G., He, X.J., Ma, X.L., Li, S., Sabel, C.E., Wang, H.K.: Impacts of O_3

600   on premature mortality and crop yield loss across China. Atmos. Environ. 194, 41-47,

601   https://doi.org/10.1016/j.atmosenv.2018.09.024, 2018.

602 Ma, Z., Hu, X., Sayer, A.M., Levy, R., Zhang, Q., Xue, Y., Tong, S., Bi, J., Huang, L., Liu, Y.: Satellite-

603   based spatiotemporal trends in $PM_{2.5}$ concentrations: China, 2004-2013. Environ. Health Per. 124,

604   184-192, https://doi.org/10.1289/ehp.1409481, 2015.

605 Malik, A., Tauler, R.: Exploring the interaction between O_3 and NO_x pollution patterns in the atmosphere

606   of Barcelona, Spain using the MCR-ALS method. Sci. Total Environ. 517, 151-161,

607   https://doi.org/10.1016/j.scitotenv.2015.01.105, 2015.

608 Marco, D.: Exposure to PM_{10}, NO_2, and O_3 and impacts on human health. Environ. Sci. Pollut. Res., 24,

609   2781, https://doi.org/10.1007/s11356-016-8038-6, 2017.

610 McPeters, R., Frith, S., Labow, G.: OMI total column ozone: extending the long-term data record. Atmos.

611   Meas. Tech. 8, 4845-4850, https://doi.org/10.5194/amt-8-4845-2015, 2015.

612 Ou, J., Zheng, J., Li, R., Huang, X., Zhong, Z., Zhong, L., Lin, H.: Speciated OVOC and VOC emission

613   inventories and their implications for reactivity-based ozone control strategy in the Pearl River Delta

614   region, China. Sci. Total Environ. 530, 393-402, https://doi.org/10.1016/j.scitotenv.2015.05.062,

615   2015.

616 Qian, M., Zhaosheng, W., Rong, W., Mei, H., Jiali, S.: Assessing the Impact of Ozone Pollution on

617   Summer NDVI based Vegetation Growth in North China. Remote Sensing Technology and

带格式的：下标

618   Application 33, 696-702, DOI: 10.11873/j.issn.1004-0323.2018.4.0696, 2018.

619   Santurtún, A., González-Hidalgo, J.C., Sanchez-Lorenzo, A., Zarrabeitia, M.T.: Surface ozone

620   concentration trends and its relationship with weather types in Spain (2001-2010). Atmos. Environ.

621   101, 10-22, https://doi.org/10.1016/j.atmosenv.2014.11.005, 2015.

622   Shang, Y., Sun, Z., Cao, J., Wang, X., Zhong, L., Bi, X., Li, H., Liu, W., Zhu, T., Huang, W.: Systematic

623   review of Chinese studies of short-term exposure to air pollution and daily mortality. Environ. Interna.

624   54, 100-111, https://doi.org/10.1016/j.envint.2013.01.010, 2013.

625   Shao, Z., Er, M.J., Wang, N.: An effective semi-cross-validation model selection method for extreme

626   learning machine with ridge regression. Neurocomputing 151, 933-942,

627   https://doi.org/10.1016/j.neucom.2014.10.002, 2015.

628   Shen, Z., Cao, J., Zhang, L., Zhao, Z., Dong, J., Wang, L., Wang, Q., Li, G., Liu, S., Zhang, Q.:

629   Characteristics of surface O_3 over Qinghai Lake area in Northeast Tibetan Plateau, China. Sci. Total

630   Environ. 500, 295-301, https://doi.org/10.1016/j.scitotenv.2014.08.104, 2014.

631   Shen, L., Jacob, D.J., Liu, X., Huang, G.Y., Li, K., Liao, H., Wang, T.: An evaluation of the ability of the

632   Ozone Monitoring Instrument (OMI) to observe boundary layer ozone pollution across China:

633   application to 2005–2017 ozone trends. Atmos. Chem. Phys. 19, 6551-6560,

634   https://doi.org/10.5194/acp-19-6551-2019, 2019.

635   Shi, X., Zhao, C., Jiang, J.H., Wang, C., Yang, X., Yung, Y.L.: Spatial Representativeness of $PM_{2.5}$

636   Concentrations Obtained Using Observations From Network Stations. J. Geophy. Res 123, 3145-

637   3158, https://doi.org/10.1002/2017JD027913, 2018.

638   Sitnov, S., Mokhov, I., Lupo, A.: Ozone, water vapor, and temperature anomalies associated with

639   atmospheric blocking events over Eastern Europe in spring-summer 2010. Atmos. Environ. 164, 180-

640 194, https://doi.org/10.1016/j.atmosenv.2017.06.004, 2017.

641 Skerlak, B., Sprenger, M., Pfahl, S., Roches, A., Sodemann, H., Wernli, H.: Rapid exchange between the

642 stratosphere and the planetary boundary layer over the Tibetan Plateau, EGU General Assembly

643 Conference Abstracts, 2014.

644 Stähle, C., Rieder, H.E., Mayer, M., Fiore, A.M.: Past and future changes in surface ozone pollution in

645 Central Europe: insights from observations and chemistry-climate model simulations, EGU General

646 Assembly Conference Abstracts, p. 12677, 2018.

647 Tan, Z., Lu, K., Jiang, M., Su, R., Dong, H., Zeng, L., Xie, S., Tan, Q., Zhang, Y.: Exploring ozone

648 pollution in Chengdu, southwestern China: A case study from radical chemistry to O_3-VOC-NO_x

649 sensitivity. Sci. Total Environ. 636, 775-786, https://doi.org/10.1016/j.scitotenv.2018.04.286, 2018.

650 Vellingiri, K., Kim, K.H., Jeon, J.Y., Brown, R.J., Jung, M.C.: Changes in NO_x and O_3 concentrations

651 over a decade at a central urban area of Seoul, Korea. Atmos. Environ. 112, 116-125,

652 https://doi.org/10.1016/j.atmosenv.2015.04.032, 2015.

653 Wang, C., Wang, X., Gong, P., Yao, T.: Polycyclic aromatic hydrocarbons in surface soil across the

654 Tibetan Plateau: Spatial distribution, source and air–soil exchange. Environ. Pollut. 184, 138-144,

655 https://doi.org/10.1016/j.envpol.2013.08.029, 2014a.

656 Wang, L., Zeng, Y., Chen, T.: Back propagation neural network with adaptive differential evolution

657 algorithm   for   time   series   forecasting.   Expert   Syst.   Appl.   42,   855-863,

658 https://doi.org/10.1016/j.eswa.2014.08.018, 2015.

659 Wang, M., Sampson, P.D., Hu, J.L., Kleeman, M., Keller, J.P., Olives, C., Szpiro, A.A., Vedal, S.,

660 Kaufman, J.D.: Combining land-use regression and chemical transport modelling in a spatiotemporal

661 geostatistical   model   for   ozone   and $PM_{2.5}$.   Environ.   Sci.   Tech.   50,   5111-5118,

662 https://doi.org/10.1021/acs.est.5b06001, 2016.

663 Wang, N., Lyu, X., Deng, X., Huang, X., Jiang, F., Ding, A.: Aggravating O_3 pollution due to NO_x

664 emission control in eastern China. Sci. Total Environ. 677, 732-744,

665 https://doi.org/10.1016/j.scitotenv.2019.04.388, 2019.

666 Wang, T., Xue, L., Brimblecombe, P., Lam, Y.F., Li, L., Zhang, L.: Ozone pollution in China: A review

667 of concentrations, meteorological influences, chemical precursors, and effects. Sci. Total Environ.

668 575, 1582-1596, https://doi.org/10.1016/j.scitotenv.2016.10.081, 2017.

669 Wang, Y., Ying, Q., Hu, J., Zhang, H.: Spatial and temporal variations of six criteria air pollutants in 31

670 provincial capital cities in China during 2013–2014. Environ. Interna. 73, 413-422,

671 https://doi.org/10.1016/j.envint.2014.08.016, 2014b.

672 Yin, P., Chen, R., Wang, L., Meng, X., Liu, C., Niu, Y., Lin, Z., Liu, Y., Liu, J., Qi, J.: Ambient ozone

673 pollution and daily mortality: a nationwide study in 272 Chinese cities. Environ. Health Per. 125,

674 117006, https://doi.org/10.1289/EHP1849, 2017a.

675 Yin, X., Kang, S., de Foy, B., Cong, Z., Luo, J., Zhang, L., Ma, Y., Zhang, G., Rupakheti, D., Zhang, Q.:

676 Surface ozone at Nam Co in the inland Tibetan Plateau: variation, synthesis comparison and regional

677 representativeness. Atmos. Chem. Phys. 17, 2017b.

678 Yoo, J.M., Lee, Y.R., Kim, D., Jeong, M.J., Stockwell, W.R., Kundu, P.K., Oh, S.M., Shin, D.B., Lee,

679 S.J.: New indices for wet scavenging of air pollutants (O_3, CO, NO_2, SO_2, and PM_{10}) by summertime

680 rain. Atmos. Environ. 82, 226-237, https://doi.org/10.1016/j.atmosenv.2013.10.022, 2014.

681 Yu, S.C., Mathur, R., Kang, D., Schere, K., Eder, B., Plein, J.: Performance and diagnostic evaluations

682 of a real-time ozone forecast by the Eta–CMAQ model suite during the 2002 New England Air

683 Quality Study (NEAQS). J. Air Waste Manage. 56, 1459-1471, 2006.

684   Yu, S.C.: Fog geoengineering to abate local ozone pollution at ground level by enhancing air moisture.

685   Environ. Chem. Lett. 17, 565-580, 2019.

686   Zang, L., Mao, F., Guo, J., Gong, W., Wang, W., Pan, Z.: Estimating hourly PM_1 concentrations from

687   Himawari-8 aerosol optical depth in China. Environ. Pollut. 241, 654-663,

688   https://doi.org/10.1016/j.envpol.2018.05.100, 2018.

689   Zang, L., Mao, F., Guo, J., Wang, W., Pan, Z., Shen, H., Zhu, B., Wang, Z.: Estimation of spatiotemporal

690   PM1. 0 distributions in China by combining $PM_{2.5}$ observations with satellite aerosol optical depth.

691   Sci. Total Environ. 658, 1256-1264, https://doi.org/10.1016/j.scitotenv.2018.12.297, 2019.

692   Zhan, Y., Luo, Y., Deng, X., Grieneisen, M.L., Zhang, M., Di, B.: Spatiotemporal prediction of daily

693   ambient ozone levels across China using random forest for human exposure assessment. Environ.

694   Pollut. 233, 464-473, https://doi.org/10.1016/j.envpol.2017.10.029, 2018.

695   Zhang, L., Jacob, D.J., Downey, N.V., Wood, D.A., Blewitt, D., Carouge, C.C., van Donkelaar, A., Jones,

696   D.B., Murray, L.T., Wang, Y.: Improved estimate of the policy-relevant background ozone in the

697   United States using the GEOS-Chem global model with 1/2×2/3 horizontal resolution over North

698   America. Atmos. Environ. 45, 6769-6776, https://doi.org/10.1016/j.atmosenv.2011.07.054, 2011.

699   Zhang, Q., Streets, D.G., He, K., Wang, Y., Richter, A., Burrows, J.P., Uno, I., Jang, C.J., Chen, D., Yao,

700   Z.: NO_x emission trends for China, 1995-2004: The view from the ground and the view from space.

701   J. Geophy. Res. 112, https://doi.org/10.1029/2007JD008684, 2007.

702   Zhang, Y., Wang, Y.: Climate-driven ground-level ozone extreme in the fall over the Southeast United

703   States. P. Natl. Acad. Sci. USA. 113, 10025-10030, https://doi.org/10.1073/pnas.1602563113, 2016.

704   Zheng, C., Shen, J., Zhang, Y., Huang, W., Zhu, X., Wu, X., Chen, L., Gao, X., Cen, K.: Quantitative

705   assessment of industrial VOC emissions in China: Historical trend, spatial distribution, uncertainties,

706   and projection. Atmos. Environ. 150, 116-125, https://doi.org/10.1016/j.atmosenv.2016.11.023, 2017.

707   Zhu, Y., Zhan, Y., Wang, B., Li, Z., Qin, Y., Zhang, K.: Spatiotemporally mapping of the relationship

708   between NO_2 pollution and urbanization for a megacity in Southwest China during 2005-2016.

709   Chemosphere 220, 155-162, https://doi.org/10.1016/j.chemosphere.2018.12.095, 2019.

710

711

712

713

Figure and table captions

Fig. 1 The geographical locations and annually mean 8-h O_3 concentrations in the ground-observed sites (red dots) over Tibetan Plateau during 2014-2018. The elevation data are collected from geographical and spatial data cloud at a 30-m spatial resolution.

Fig. 2 The workflow for predicting the spatiotemporal distributions of 8-h O_3 levels.

Fig. 3 Density scatterplots of model fitting and cross-validation result at a daily level. (a), (b), and (c) represent RF-GAM, RF-STK, and RF models, respectively. The red dotted line denotes the fitting linear regression line. The full names of MPE and RMSE are mean prediction error ($\mu g/m^3$) and root mean squared prediction error ($\mu g/m^3$), respectively.

Fig. 4 The transferring ability validation of RF-GAM method based on the measured daily 8-h O_3 concentration during December 2013-May 2014.

Fig. 5 The variable importance of predictors in the final RF-GAM model.

Fig. 6 The mean value of estimated 8-h O_3 concentration during 2005-2018 over Tibetan Plateau.

Fig. 7 The inter-annual variation of predicted 8-h O_3 level ($\mu g/m^3$) from 2005 to 2018 across Tibetan Plateau.

Fig. 8 The trend analysis of predicted 8-h O_3 concentration. (a) and (b) represent the result of Mann-Kendall method and discrepancy of estimated O_3 level during 2005-2018 across Tibetan Plateau.

Fig. 9 The seasonal variability of estimated 8-h O_3 level across Tibetan Plateau. (a), (b), (c), and (d) represent the predicted 8-h O_3 concentrations in spring, summer, autumn, and winter, respectively.

Fig. 10 The spatial distributions of nonattainment days in Tibetan Plateau during 2005-2018.

Table 1 The R^2 values, RMSE, MPE, and RPE of RF-GAM in different years during 2014-2018 over Tibetan Plateau.

Table 2 The R^2 values, RMSE, ~~and~~ MPE, and RPE of RF-GAM in four seasons over Tibetan Plateau.

Table 3 The predictive performances ~~R^2 values, RMSE, and MPE~~ of RF-GAM in different provinces over Tibetan Plateau.

Table 4 The estimated 8-h O$_3$ concentration in 19 prefecture-level cities over Tibetan Plateau during four seasons including spring, summer, autumn, and winter.

Table 5 The mean nonattainment days (8-h O$_3$ level >100 μg/m^3) in 19 prefecture-level cities over Tibetan Plateau each year.

Fig. 1
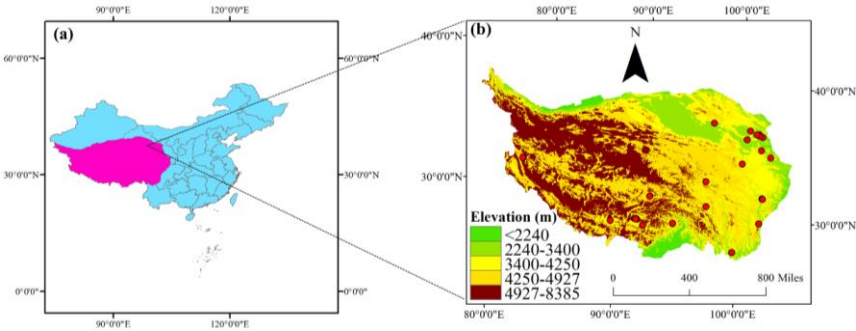
Fig. 2
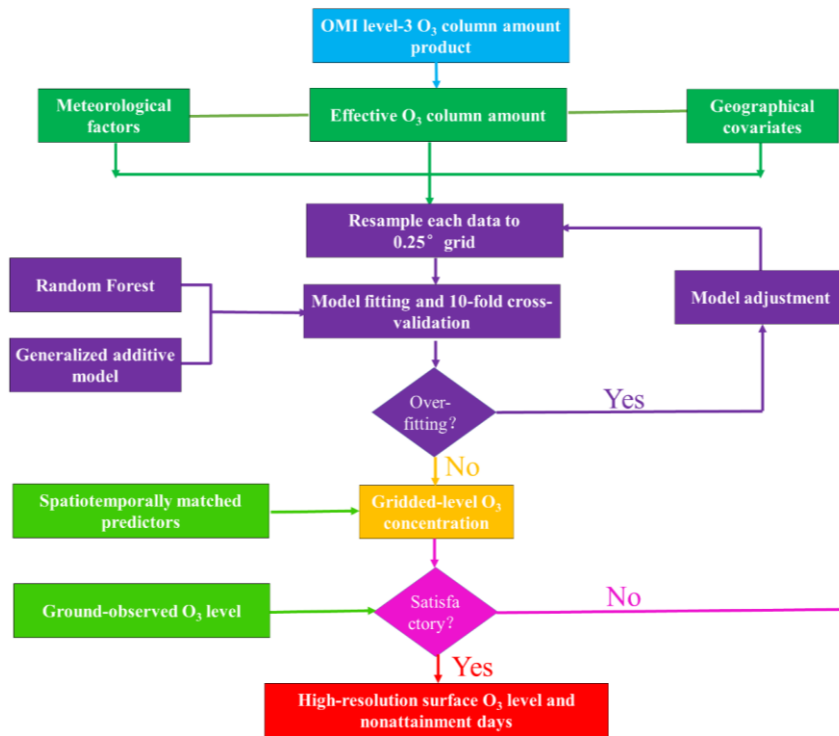
Fig. 3
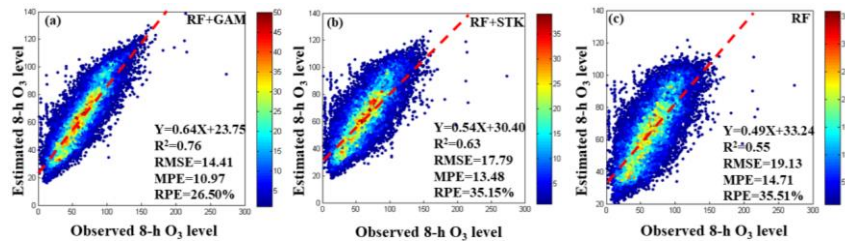
Fig. 4
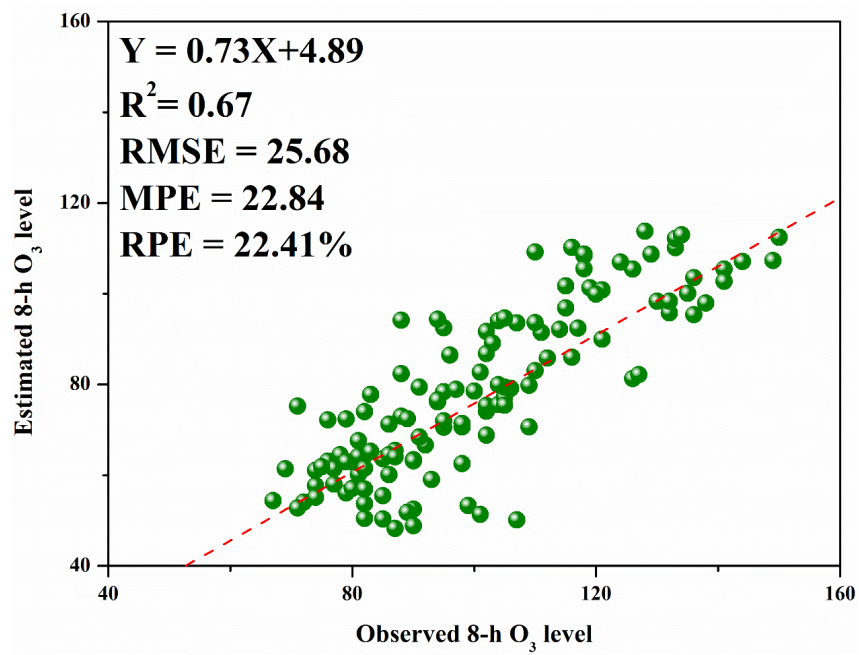
Fig. 5
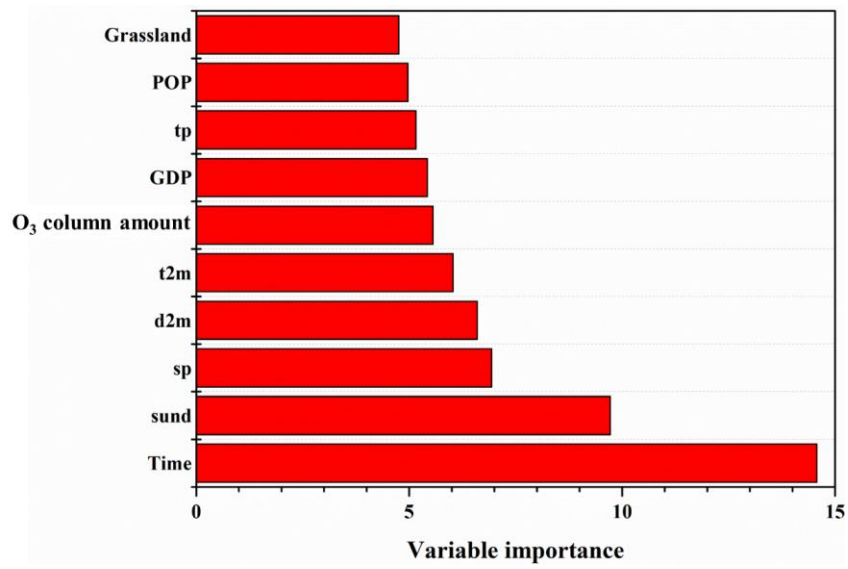
Fig. 6
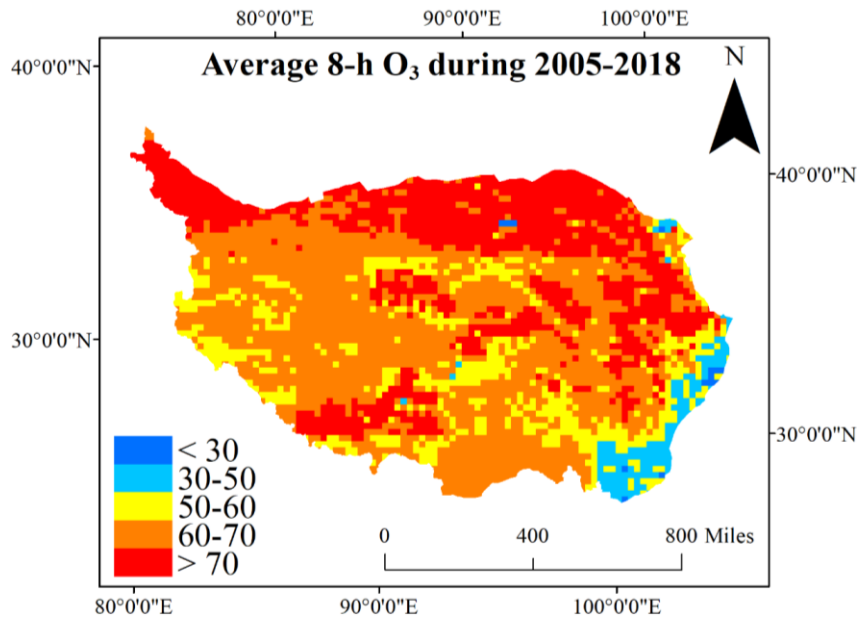
Fig. 7
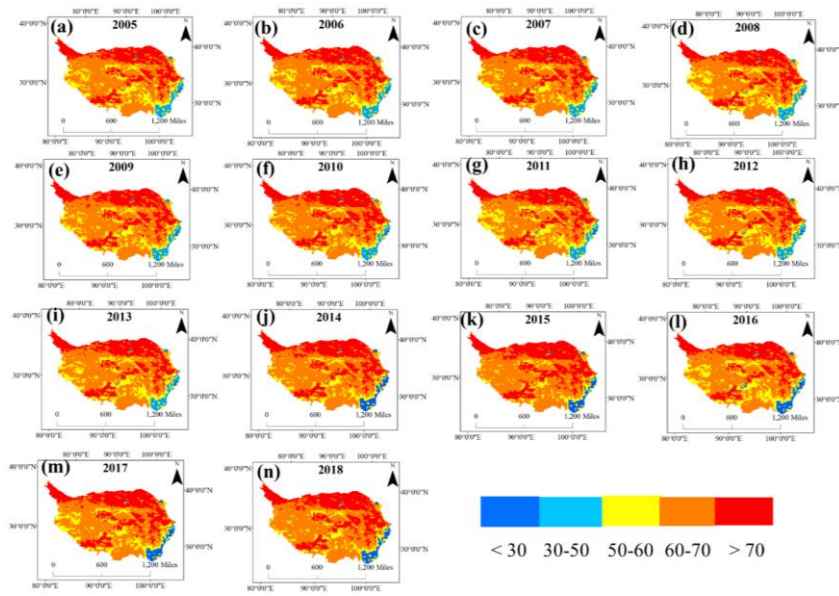
Fig. 8
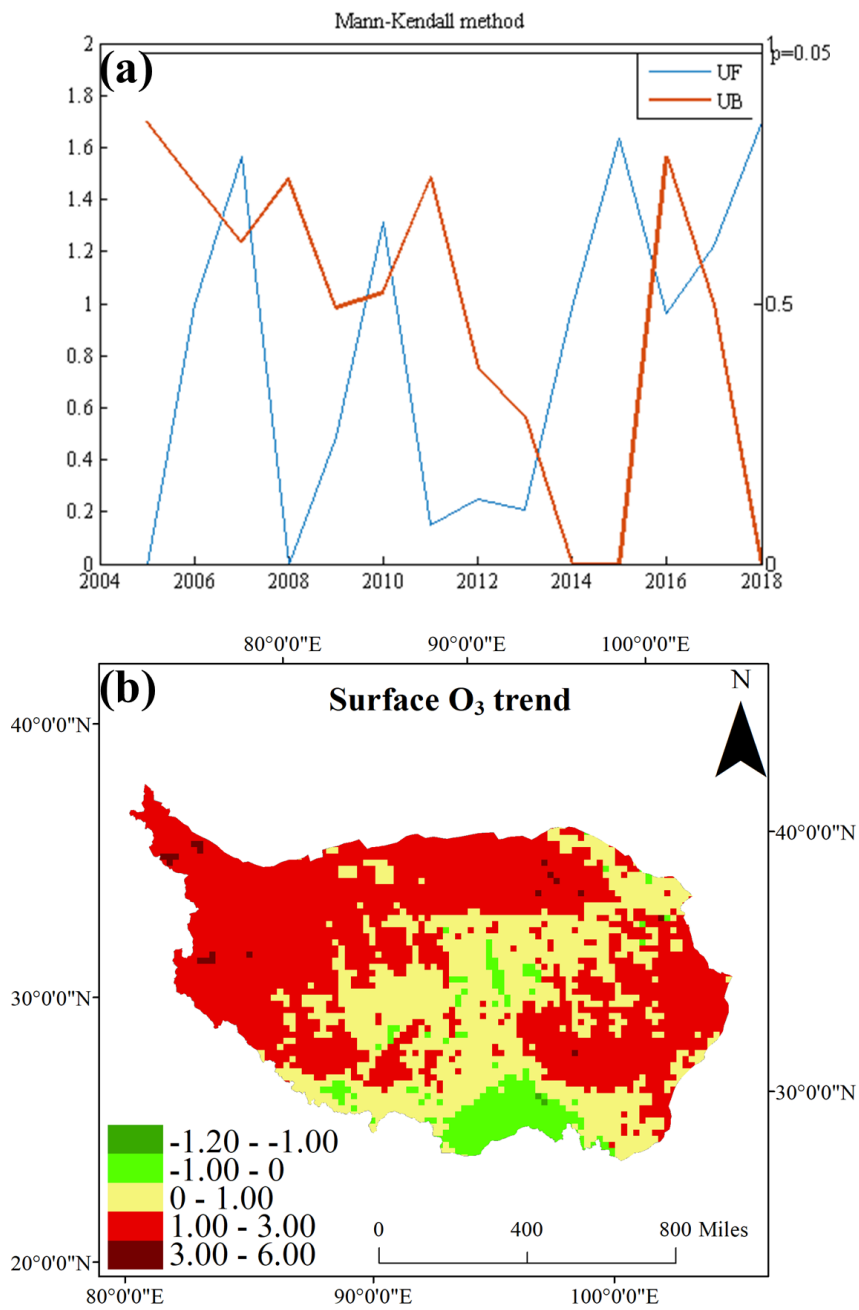
Fig. 9
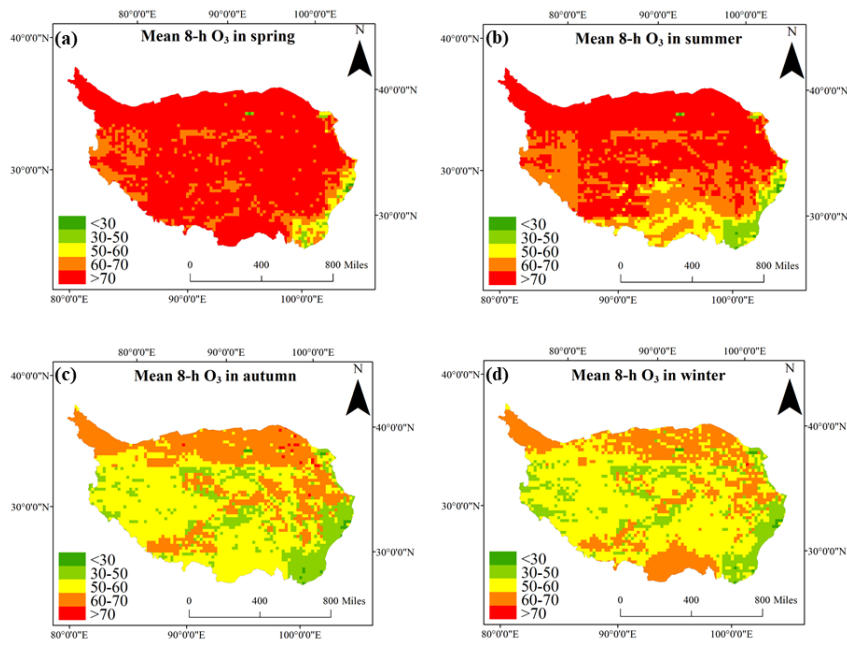
Fig. 10
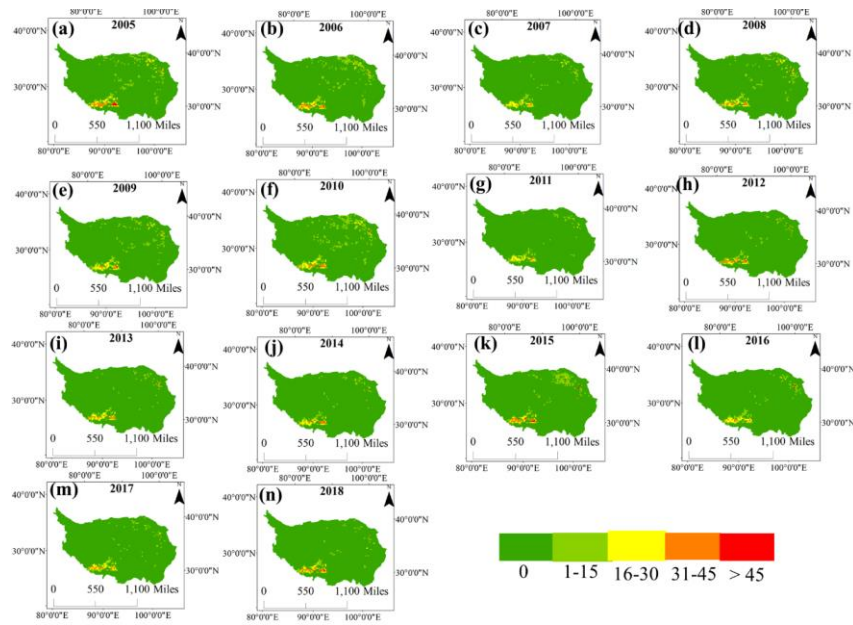
Table 1

	2014	2015	2016	2017	2018
R^2	0.69	0.72	0.76	0.73	0.75
RMSE	13.65	14.56	14.28	14.52	14.35
MPE	9.53	10.82	10.84	10.95	10.93
RPE	23.27%	23.26%	23.02%	23.20%	23.09%

Table 2

	Spring	Summer	Autumn	Winter
R^2	0.64	0.74	0.67	0.69
RMSE	15.32	15.13	13.23	14.58
MPE	11.94	11.75	10.52	11.44
RPE	24.63%	22.35%	23.32%	23.24%

Table 3

	Tibet	Qinghai	Gansu	Sichuan	Yunnan
R^2	0.69	0.70	0.74	0.71	0.54
RMSE	14.81	14.83	13.65	13.23	12.49
MPE	11.24	11.33	10.88	10.08	10.20
RPE	22.90%	22.65%	22.51%	22.62%	25.85%

Table 4

	Province	Spring	Summer	Autumn	Winter	Annual	Measured O_3 level
Aba	Sichuan	65.61±14.30	59.46±14.32	45.55±12.03	47.95±10.55	55.17±12.77	47.75±19.47
Ngari	Tibet	71.34±3.12	70.10±3.57	53.14±3.67	51.84±3.69	62.21±3.34	53.34±24.46
Qamdo	Tibet	72.52±4.29	62.74±5.79	52.06±4.01	55.42±3.09	61.10±3.93	59.76±23.77
Diqing	Yunnan	56.38±7.87	44.35±5.90	37.45±5.76	45.88±7.05	46.22±6.51	47.81±21.63
Gannan	Gansu	76.77±9.73	73.27±10.67	54.74±8.33	54.72±6.95	65.60±8.91	68.86±25.45
Ganzi	Sichuan	69.38±10.99	61.45±11.58	48.49±8.79	50.94±6.62	58.06±9.48	38.07±19.08
Guoluo	Qinghai	80.12±5.12	76.13±5.83	58.86±5.71	57.38±4.66	68.77±5.25	80.04±23.90
Haibei	Qinghai	78.18±10.21	78.84±10.31	60.90±9.69	57.48±9.78	69.47±9.99	81.07±32.74
Haidong	Qinghai	74.20±10.34	73.70±9.12	53.61±8.11	51.02±9.60	63.84±9.21	44.28±34.96
Hainan	Qinghai	83.01±5.36	82.27±5.72	61.57±5.39	58.96±5.44	72.24±5.34	78.34±27.11
Haixi	Qinghai	79.39±6.88	79.48±7.79	60.78±7.48	57.71±6.99	69.99±7.24	80.60±27.17
Huangnan	Qinghai	85.21±4.98	83.01±4.66	61.95±4.18	60.62±4.49	73.48±4.53	74.83±22.63
Lhasa	Tibet	80.08±9.63	70.13±8.42	55.86±5.78	55.85±5.19	65.99±7.24	75.45±26.65
Nagqu	Tibet	74.59±5.13	70.46±6.69	54.60±5.16	53.53±4.83	63.83±5.23	44.79±28.75
Shigatse	Tibet	77.31±8.62	69.66±7.69	55.93±4.58	55.57±4.72	65.15±6.14	75.62±26.50
Sannan	Tibet	73.90±5.97	61.00±5.86	54.70±3.13	61.71±4.32	63.04±4.00	73.04±26.31
Xining	Qinghai	77.43±10.27	77.84±9.44	58.19±9.29	54.72±10.04	67.77±9.70	61.77±22.58
Yushu	Qinghai	77.35±5.55	73.34±6.37	56.12±5.53	55.02±5.01	66.05±5.50	57.14±31.98
Nyingchi	Tibet	73.22±2.77	59.60±2.33	53.84±2.06	62.24±3.63	62.40±2.20	66.61±26.71

Table 5

	Spring	Summer	Autumn	Winter	Annual
Aba	0	0	0	0	0
Ngari	0	0	0	0	0
Qamdo	0	0	0	0	0
Diqing	0	0	0	0	0
Gannan	0	1	0	0	1
Ganzi	13	2	0	0	15
Guoluo	19	21	0	0	40
Haibei	0	0	0	0	0
Haidong	22	18	0	0	40
Hainan	14	12	1	0	27
Haixi	1	1	0	0	2
Huangnan	23	22	0	0	45
Lhasa	12	7	0	0	19
Nagqu	24	14	0	0	38
Shigatse	28	13	0	0	41
Sannan	33	7	0	0	40
Xining	2	1	0	0	3
Yushu	0	0	0	0	0
Nyingchi	0	0	0	0	0